ImmunoHorizons

RESEARCH ARTICLE

Infectious Disease

B Cell Chronic Lymphocytic Leukemia Development in Mice with Chronic Lung Exposure to *Coccidioides* Fungal Arthroconidia

Vanessa Coyne, Heather L. Mead, Patricia K. A. Mongini,[1] and Bridget M. Barker[1]

Pathogen Microbiome Institute, Northern Arizona University, Flagstaff, AZ

ABSTRACT

Links between repeated microbial infections and B cell chronic lymphocytic leukemia (B-CLL) have been proposed but not tested directly. This study examines how prolonged exposure to a human fungal pathogen impacts B-CLL development in Eμ-hTCL1–transgenic mice. Monthly lung exposure to inactivated *Coccidioides* arthroconidia, agents of Valley fever, altered leukemia development in a species-specific manner, with *Coccidioides posadasii* hastening B-CLL diagnosis/progression in a fraction of mice and *Coccidioides immitis* delaying aggressive B-CLL development, despite fostering more rapid monoclonal B cell lymphocytosis. Overall survival did not differ significantly between control and *C. posadasii*–treated cohorts but was significantly extended in *C. immitis*–exposed mice. In vivo doubling time analyses of pooled B-CLL showed no difference in growth rates of early and late leukemias. However, within *C. immitis*–treated mice, B-CLL manifests longer doubling times, as compared with B-CLL in control or *C. posadasii*–treated mice, and/or evidence of clonal contraction over time. Through linear regression, positive relationships were noted between circulating levels of $CD5^+/B220^{low}$ B cells and hematopoietic cells previously linked to B-CLL growth, albeit in a cohort-specific manner. Neutrophils were positively linked to accelerated growth in mice exposed to either *Coccidioides* species, but not in control mice. Conversely, only *C. posadasii*–exposed and control cohorts displayed positive links between $CD5^+/B220^{low}$ B cell frequency and abundance of M2 anti-inflammatory monocytes and T cells. The current study provides evidence that chronic lung exposure to fungal arthroconidia affects B-CLL development in a manner dependent on fungal genotype. Correlative studies suggest that fungal species differences in the modulation of nonleukemic hematopoietic cells are involved. *ImmunoHorizons*, 2023, 7: 333–352.

INTRODUCTION

B cell chronic lymphocytic leukemia (B-CLL) is a malignancy of the $CD5^+$ B-1 subset of B lymphocytes and the most frequent adult leukemia in the United States and Western Europe. The malignancy appears with advancing age and has a lifetime risk of 0.57% (https://www.cancer.org/cancer/chronic-lymphocytic-leukemia/about/key-statistics). Leukemic transformation is typically preceded for several years by monoclonal B cell lymphocytosis (MBL), a condition in which the frequency of blood $CD5^+$ B cells is chronically elevated above normal (1). Even prior to MBL and up to 16 y before B-CLL diagnosis, a dominant high-risk B cell IgH (IgVH) clonotype is detectable (2). Leukemic cells in blood are relatively quiescent, but significant clonal growth occurs in

Received for publication March 1, 2023. Accepted for publication April 24, 2023.

Address correspondence and reprint requests to: Dr. Patricia K. A. Mongini, Pathogen Microbiome Institute, Northern Arizona University, 1395 S Knowles Drive/Building 56/STE 210, Flagstaff, AZ 86001. E-mail address: patricia.mongini@nau.edu

[1]P.K.A.M. and B.M.B. are cosenior authors.

ORCIDs: 0000-0002-5680-0758 (H.L.M.); 0000-0002-4966-7741 (P.K.A.M.); 0000-0002-3439-4517 (B.M.B.).

This work was supported by the Northern Arizona University Foundation.

V.C. managed the in vitro growth, isolation, and fixation of *Coccidioides* arthroconidia, kept records of all mice used for these experiments, administered arthroconidia via the intranasal route, performed all blood collections, monitored mice for survival endpoint, performed euthanasia and necropsies, and contributed to the manuscript; H.L.M. was instrumental in training V.C. in all class II biological safety cabinet procedures involving manipulation of *Coccidioides* and in guiding early mouse manipulations; P.K.A.M. initiated the hypothesis, developed the project with B.M.B., managed all blood cell enumeration/staining, flow cytometric analyses, and data computation, and wrote the manuscript; and B.M.B. developed the project with P.K.A.M. and was responsible for coordinating all efforts involving *Coccidioides* and animal manipulation and helped write the manuscript.

Abbreviations used in this article: AICDA, activation-induced cytosine deaminase; B-CLL, chronic lymphocytic leukemia; DT, doubling time; MBL, monoclonal B cell lymphocytosis; NET, neutrophil extracellular trap; PAMP, pathogen-associated molecular pattern; Tg, transgenic.

The online version of this article contains supplemental material.

lymphatic tissues (3–6). Whereas B-CLL is often characterized by slow growth, warranting a "wait-and-watch" approach to therapy, malignant clones can become aggressive. This reflects the emergence of variant cells bearing new single-point mutations or deletions (7, 8) and changes in their growth-supporting milieu (9).

Nontransformed B-1 B cells have important roles both in early Ab responses to bacterial, viral, and fungal pathogens (10–13) and in synthesis of Abs that clear the body of apoptotic/stressed cells (14). Correspondingly, the BCRs on these B-1 cells are typically polyreactive, enabling their engagement with both microbes and compromised cells (15). While B-1 cells spontaneously produce Ab, as a form of innate immunity (16), microbes can also elicit their clonal expansion (10, 15, 17).

A link between infections and B-CLL development has been long suspected. First, the IgVH/IgVL repertoire of leukemic clones is highly skewed and shared by unrelated patients and mice (3, 18–22). Although BCRs of many B-CLL populations can engage both microbes and self-epitopes (23–26), in some clones, BCR specificity for infectious agents is dominant. The latter is exemplified by a subset of IgVH-mutated B-CLLs with high affinity for fungal β-glucan (18) that are selectively activated in vitro by fungal products (18). Second, several epidemiological studies reveal a statistical link between repeated infections and later B-CLL emergence (27, 28). Third, lymph nodes (LNs) that drain infected tissues and harbor microbes (29) are major sites for B-CLL clonal expansion in patients. Microbe-elicited TLR signaling may be a major driver for this clonal expansion, as suggested by gene expression profiles of proliferating B-CLL cells within LNs (30), the typically elevated B-CLL expression of TLRs for microbe-expressed pathogen-associated molecular patterns (PAMPs) (31, 32), and the often significant in vitro B-CLL clonal expansion elicited upon coculture with ligands for TLR9 (or TLR2) and cytokines typical of inflamed tissues (5) (P.K.A.M., unpublished observations). Notwithstanding, it is still a conjecture that infection drives the transformation process and/or B-CLL growth in patients.

Using an approach possible only with experimental animals, the current study employs Eμ-hTCL1–transgenic (Tg) mice (33) (hereafter termed TCL1-Tg mice) to test whether chronic lung exposure to an airborne fungus, *Coccidioides*, influences the temporal appearance and/or progression of B-CLL. These mice have been extensively used as a model for human B-CLL since their development by Bichi et al. (33, 34). Virtually all untreated TCL1-Tg mice develop B-CLL with advanced age, with a time course that varies between individuals (33, 35).

Coccidioides immitis and *Coccidioides posadasii,* etiologic agents for Valley fever, are dimorphic fungi endemic to the western United States and regions of Mexico, Central America, and South America (36, 37). Within arid soils, *Coccidioides* replicates in its mycelial form, generating arthroconidia that are released into the environment (37). Upon inhalation into lungs, conidia transform into spherules, the parasitic form of *Coccidioides*. Immature spherules enlarge, undergo numerous nuclear divisions, and form hundreds of endospores that are released upon rupture of the mature spherule. Diffusing endospores mature into new spherules, repeating the above process (38).

Prior studies in mice exposed to in vitro–propagated *Coccidioides* arthroconidia show that the immune system responds with rapid mobilization of neutrophils and macrophages, followed by a strong Ab response thought to be poorly protective (39), and the activation of various T cell subsets, both inflammatory and anti-inflammatory (40, 41). Histological examinations of lungs from arthroconidia-exposed mice and patients with Valley fever show that a localized granuloma is formed by incoming neutrophils with macrophages and lymphocytes at the periphery (41, 42). In humans, an abundance of IL-10^{+} B cells within surrounding lymphocyte clusters (41) suggests the participation of regulatory B cells (43, 44). Most *Coccidioides* infections resolve within weeks, but a considerable proportion can become chronic, with occasional dissemination to other organs/tissues (45–47).

In endemic areas, both *C. posadasii and C. immitis* are major causes of community-acquired pneumonia (48) that is rising with climate change (37). *C. immitis* predominates in California, and *C. posadasii* is most prevalent in Arizona, New Mexico, and Texas (49). The two species appear to have diverged ∼5 million years ago (50) and exhibit several genetic differences (46). To date, no straightforward evidence has emerged of differing disease manifestations by the two species, albeit an earlier mouse study found significant differences between the *C. posadasii* and *C. immitis* strains in eliciting several inflammatory proteins at 3–5 d after lung infection (51).

The following study compares the age of B-CLL diagnosis, in vivo leukemic cell doubling times (DTs), and mouse survival in control TCL1-Tg mice and TCL1-Tg mice chronically exposed to formalin-inactivated *C. posadasii* or *C. immitis* arthroconidia. We report that leukemia-prone mice exposed to either species of *Coccidioides* exhibit elevated blood levels of neutrophils, T cells, and B cells (conventional and B-1) prior to leukemia diagnosis, consistent with an activated immune system. However, important differences between the two *Coccidioides* species exist, both in the relative effect on B-CLL development and relative correlation of ancillary leukocyte subsets in blood with circulating frequency of CD5^{+}/B220^{low} (preleukemic and leukemic) B cells.

MATERIALS AND METHODS

Experimental mice

Breeding pairs for homozygous Eμ-hTCL1–Tg mice, backcrossed on the C57BL/6 background, were provided by Drs. Nicholas Chiorazzi and Xiao Yan (Feinstein Institute for Medical Research/Northwell Health, Manhasset, NY) (21) upon the approval of Dr. Carlo Croce, whose laboratory developed and characterized mice with the Eμ-hTCL1 transgene (33, 52). TCL1-Tg/C57BL/6 mice were expanded at Northern Arizona University in its American Association of Laboratory Animal Care–accredited animal facility. Presence of the human TCL1 transgene

was confirmed by PCR using specific primers (forward, 5′-GCCGAGTGCCCGACACTC-3′; reverse, 5′-AGACCCCAGATCCAGAAAGG-3′) (https://www.ncbi.nlm.nih.gov/gene/8115). Mice were maintained at the animal care facility at Northern Arizona University under protocol numbers 17-012 and 21-011.

At the time of weaning (3 wk), mice from each litter were divided among three experimental cohorts, with males and females equally represented in each cohort. Each individually ventilated cage contained from one to a maximum of five mice, with numbers largely dependent on whether male mice were littermates. Experimental cohorts were established on the basis of monthly treatments: PBS cohort, 14 mice; arthroconidia-exposed cohorts, 17 mice with $n = 9$ exposed to *C. posadasii* (SILV) and $n = 8$ exposed to *C. immitis* (RS). Intranasal administration began at 1 mo of age and continued monthly throughout the lifespan of each mouse. Beginning at 5–6 mo of age, blood samples were collected monthly, at 7–10 d following the intranasal treatment.

Preparation of Coccidioides *conidia for intranasal inhalation*

In vitro–propagated *Coccidioides* strains (SILV and RS) (53) were cultured on solid media (1% yeast extract, 2% glucose, and 1.5% agar), grown for 6 wk, and harvested following methods in Mead et al. (54). Harvested conidia were exposed to 1% PBS-buffered formalin for 48 h. Fixed conidia were washed and stored at 4°C up to 4 mo, and then refreshed using the same protocol. Sterility checks were conducted on wild-type strains prior to bringing samples out of the biosafety level 3 laboratory to ensure that all organisms were killed with the procedure. For intranasal inhalation, animals were lightly anesthetized with isoflurane and exposed to 30 μl of 500 arthroconidia in PBS, following the protocols detailed in Mead et al. (54).

WBC enumeration and immunofluorescent staining for phenotypic markers

Blood was collected from the submandibular vein following isoflurane anesthesia into EDTA-coated microfuge tubes with rapid mixing (https://lists.purdue.edu/pipermail/cytometry/2002-March/021840.html). All samples were stored on ice and processed within 3 h of collection. The volume of blood in each microfuge collection tube was determined following a few seconds of rapid microfuge centrifugation and recorded. Following dilution with cold PBS, centrifugation, and removal of the plasma-rich layer, the cell pellet was treated for 4–5 min with cold 1× RBC lysis buffer (BioLegend, San Diego, CA) before additional centrifugation, washing of the pellet in cold PBS, and resuspension in assay buffer (PBS + 1% BSA + 0.1% sodium azide). An aliquot of cells was used to obtain a WBC count by hemocytometer (in duplicate) and the total WBCs/ml collected blood was calculated.

Remaining cells were used for immunofluorescence staining, unless the WBC count exceeded ∼20 million/ml blood, in which case cells were diluted in assay buffer to obtain <1 million cells per staining well. Before exposure to fluorochrome-conjugated Abs, cells were pretreated for 15 min with TruStain FcX (anti-mouse CD16/32 blocking Ab; BioLegend, 101319). Subsequently, WBCs from each blood sample were stained separately for 1) $CD45^+$ B cells, B-CLL cells, and T cells and 2) $CD45^+$ neutrophils, total monocytes, and monocyte M1 and M2 subsets, with staining typically performed in duplicate. The frequency of each population in blood (millions/ml) was determined from its proportional representation in the WBC population by flow cytometry and the total WBC count/ml blood, determined as above. Fluorochrome-conjugated Abs used for these determinations were specific for the following: B220-AF488 (BD Pharmingen, 557669), CD5-PE (BD Pharmingen 553023, clone 53-7.3), CD19-allophycocyanin (BioLegend, clone 1B3), CD45-PerCP-Cy5.5 (BD Biosciences, 550994), CD11b-allophycocyanin (clone M1/70, BioLegend), Ly6G-allophycocyanin-eBio780 (eBioscience, clone 1AB-Ly6G; Invitrogen, 47-9668-80), CD115-PE (BioLegend, 135506, clone AFS98), and Ly6C-AF488 (BioLegend, 128021, clone HK1.4). Control IgG Abs included the following: FITC-mouse IgG2a (BD Biosciences, clone G20-127), PE–rat IgG2b (R&D Systems, IC013P), PerCP mouse IgG1 (BD Biosciences, 349044), and allophycocyanin–mouse IgG1 (R&D Systems, 1C002A). Staining of cells involved a 30-min incubation at 4°C with the relevant Ab-staining mixture in assay buffer, and a subsequent three washes in cold assay buffer, followed by one wash in cold PBS and fixation in 1.5% EM-grade paraformaldehyde in PBS. Flow cytometric evaluation of stained cells was performed with a dual-laser Beckman Coulter CytoFLEX flow cytometer, with single-color compensation tubes prepared by incubating One-Comp eBeads compensation beads (Invitrogen, 01-1111) with either Ly6C-AF488, CD5-PE, CD45-PerCP-Cy5.5, CD19-allophycocyanin, or Ly6G-allophycocyanin-eBio780. Data analysis was performed with FlowJo.

Criteria for diagnosis of MBL, B-CLL, and transformation into "overt" B-CLL

MBL was diagnosed when frequency of blood $CD5^+B220^{low}$ B cells reached 0.5 to >5 million cells/ml. B-CLL was diagnosed when the frequency of blood $CD5^+B220^{low}$ B cells was ≥5 million cells/ml in three consecutive blood samples, or, alternatively, when the last blood sample taken prior to a survival endpoint contained >10 million $CD5^+B220^{low}$ B cells/ml. Conversion into overt B-CLL was determined when the blood frequency of $CD5^+B220^{low}$ B cells reached ≥20 million cells/ml.

B-CLL in vivo DT

B-CLL DT (in days) for each B-CLL population was determined from peripheral blood frequencies of $CD5^+B220^{low}$ B cells over sequential months. For DT determinations, an online DT/growth rate calculator based on exponential regression was used (http://www.doubling-time.com/compute.php). In a prior study, the latter was employed to monitor in vivo growth rate of human B-CLL populations (5).

https://doi.org/10.4049/immunohorizons.2300013

Survival endpoint determinations

Early during this study, overall health of mice was monitored daily. Following 7–8 mo of age, mice were checked twice daily for physical changes. Although occasional mice died prior to significant physical signs of decline, in most cases mice reaching criteria for a survival endpoint were euthanized. This was characterized by labored breathing, lack of appetite, poor body condition, and lack of movement after stimulus, and typically confirmed by the animal facilities veterinarian.

Necropsy determinations

Euthanized mice, or in rare cases mice that died spontaneously within a day after the last inspection, were subjected to necropsy. Necropsies were performed by the same individual in nearly all cases and included measurement of spleen length (in centimeters) and subjective determination of relative enlargement (lymphadenopathy) of thoracic lymph LNs and inguinal LNs. Additionally, the condition of lungs and liver was noted. Although initial necropsy tissues were not photographed, those from nearly all later necropsies were. This allowed for independent tissue assessments by two additional investigators, and in these cases, tissue enlargement scores reflected the mean assessments of the three investigators.

Statistical analysis

Pairwise comparisons of parametric data from two independent cohorts involved the two-sided, unpaired *t* test, or when data were nonparametric, the Mann–Whitney *U* test. Insights into whether the three experimental cohorts exhibited statistically significant differences involved the Kruskal–Wallis one-way ANOVA on ranks, followed by pairwise multiple comparisons (Dunn's method). Kaplan–Meier plots were used to assess whether the time course for emergence of B-CLL, or overt B-CLL, differed between the three experimental cohorts, with statistical significance determined by a log-rank analysis. When statistical differences were present by the latter, pairwise comparisons for statistical significance employed the Holm–Sidak method. Kaplan–Meier plots with log-rank/Holm–Sidak statistical analyses were also employed to compare overall survival and disease-specific survival within the three cohorts. Disease-specific survival compared the longevity of mice diagnosed with B-CLL. Linear regression analyses assessed for statistically significant relationships between frequencies of $CD5^+B220^{low}$ B cells and possible ancillary populations of WBCs. Regression plots yielding p values <0.05 were considered statistically significant. All statistical analyses were performed with SigmaPlot software.

RESULTS

Experimental design and blood leukocyte gating

Fig. 1 outlines this study's approach for testing the hypothesis that repeated lung exposure to *Coccidioides* fungal arthroconidia accelerates B-CLL emergence and/or aggressiveness. Lung exposure was achieved through monthly intranasal administration of fixed *C. posadasii* (SILV) or *C. immitis* (RS) arthroconidia, beginning at ∼1 mo of age (Fig. 1A). Monthly blood samples from fungus-treated and PBS-treated control mice were collected beginning at 5–6 mo, an age prior to leukemia manifestation in most TCL1-Tg mice (33). Following immunofluorescence staining, the indicated flow cytometric gating strategies (Fig. 1B, 1C) were used to assess the proportions of B cells with leukemic phenotype ($CD19^+$, $CD5^+$, $B220^{low}$) and other leukocytes within $CD45^+$ gated WBCs (normal B and T cells, neutrophils, and monocytes). Population frequency was calculated from numbers of total WBCs/ml blood (found by hemocytometer cell count) and each population's representation within total WBCs.

Altered blood leukocyte levels in Coccidioides*-exposed TCL1-Tg mice at 6–7 mo of age*

In the earliest blood samples, we found several leukocyte populations elevated in *Coccidioides*-exposed cohorts, as compared with PBS-treated control mice. Data in Fig. 2A show that neutrophil frequency was higher in both SILV- and RS-treated cohorts, as compared with the control group, with statistical significance reached only in the RS-treated cohort ($p = 0.02$). Additionally, both SILV- and RS-treated mice manifested significantly greater frequencies of total T cells (Fig. 2B) and total B cells (Fig. 2C) than did control mice. Furthermore, the levels of conventional B cells ($CD5^-/B220^{high}$) were significantly higher in RS-treated mice than in controls ($p = 0.04$) (Fig. 2D). Finally, significantly elevated frequencies of $CD5^+/B220^{low}$ B-1 cells (Fig. 2E) were found in RS-treated mice as compared with controls ($p = 0.01$), although neither RS mice nor control mice reached a threshold for tentative B-CLL diagnosis (≥5 million/ml). Although two of nine (22%) SILV-treated mice did manifest ≫5 million $CD5^+/B220^{low}$ B cells at this age, the mean frequency of $CD5^+/B220^{low}$ B cells in the latter cohort did not differ significantly from control mice. At ages >7 mo, greater intracohort variability was noted in all cell populations, and no statistically significant differences between cohorts were found (Supplemental Fig. 1 and data not shown). Taken together, these findings indicate that chronic lung exposure to *Coccidioides* conidia elevates the levels of several distinct blood leukocyte lineages, generally prior to the emergence of B-CLL, with the exception of two mice in the SILV-treated cohort.

B-CLL development in control and Coccidioides*-exposed TCL1-Tg mice*

Histograms in Fig. 3 show the frequencies of $CD5^+/B220^{low}$ B cells (preleukemic and leukemic) across the lifespan of individual mice within each cohort. Consistent with past studies (33), the time course for B-CLL appearance in TCL1-Tg mice was highly variable. During the ∼15-mo duration of this experiment, overall B-CLL incidence in the PBS, SILV, and RS-treated cohorts was 36, 56, and 63 percent, respectively, and incidence of overt B-CLL was 14, 33, and 38 percent, respectively (Fig. 3A–C). Although not all mice were diagnosed with B-CLL prior to their endpoint,

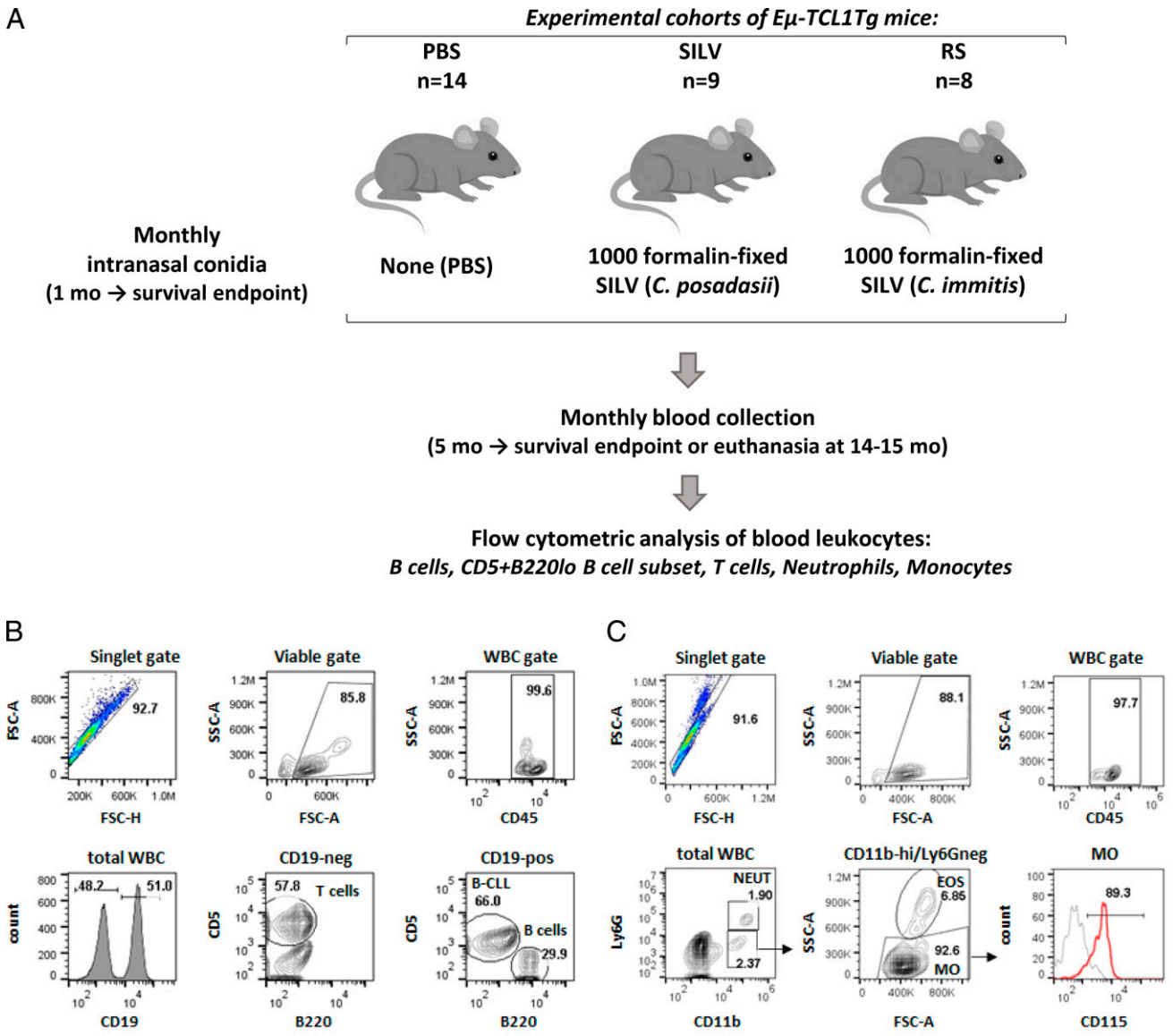

FIGURE 1. Experimental design and gating strategy for diverse blood leukocytes.

(**A**) With three cohorts of B-CLL–prone TCL1-Tg mice, we examined whether B-CLL development is affected by repeated inhalation of *Coccidioides* arthroconidia. The control cohort was exposed to vehicle alone (PBS; $n = 14$); test cohorts received 1000 fixed *C. posadasii* conidia (SILV; $n = 9$) or 1000 fixed *C. immitis* conidia (RS; $n = 8$) monthly, beginning at ~1 mo of age and continuing throughout each recipient's lifespan. Blood samples were acquired monthly, beginning at 5–6 mo. Total WBCs in individual samples were counted and normal and leukemic cells were distinguished by immunofluorescence staining and flow cytometry. (**B**) Gating strategy for B and T lymphocytes. Viable singlets were gated for the pan-leukocyte marker, CD45, and assessed for CD19 expression. T cells within the $CD19^-$ population were identified by their $CD5^{high}$ status. Normal and leukemic B cells within the $CD19^+$ gate were distinguished as follows: B-CLL cells, $CD5^+/B220^{low}$; normal B cells, $CD5^-/B220^{high}$. (**C**) Neutrophils and monocytes. Viable singlets, gated for CD45, were evaluated for CD11b and Ly6G expression. Neutrophils are $Ly6G^+/CD11b^{high}$; monocyte-enriched WBCs are $Ly6G^-/CD11b^{high}$. Contaminating eosinophils were removed from the latter by gating out cells with high side scatter (SSC). The resulting monocyte population ($Ly6G^-/CD11b^{high}/SSC^{low}$) expressed CD115, a marker of blood monocytes. Note that in most mice ≤7 mo of age, monocytes were not enumerated due to suboptimal monocyte staining/gating, and neutrophils were gated either as $CD45^+CD19^-CD5^-/SSC^{high}$ or as $CD45^+/Ly6G^+$. Later comparisons indicated that the latter two approaches at neutrophil enumeration yielded results highly concordant with neutrophils gated as $CD45^+/CD11b^{high}/Ly6G^+$ (C).

$CD5^+/B220^{low}$ B cells represented >35% of total circulating B cells within the last blood sample taken, in all but 4 of 31 total mice (87%) (Supplemental Fig. 1). In this last blood sample, the mean ± SD values for the percent $CD5^+/B220^{low}$ B cells within control, SILV-, and RS-treated cohorts were 66.3 ± 29.9, 65.8 ± 34.4, and 83.2 ± 16.1%, respectively.

Temporal monitoring of $CD5^+B220^{low}$ B cell frequencies during the lifespan of individual mice further emphasizes these

https://doi.org/10.4049/immunohorizons.2300013

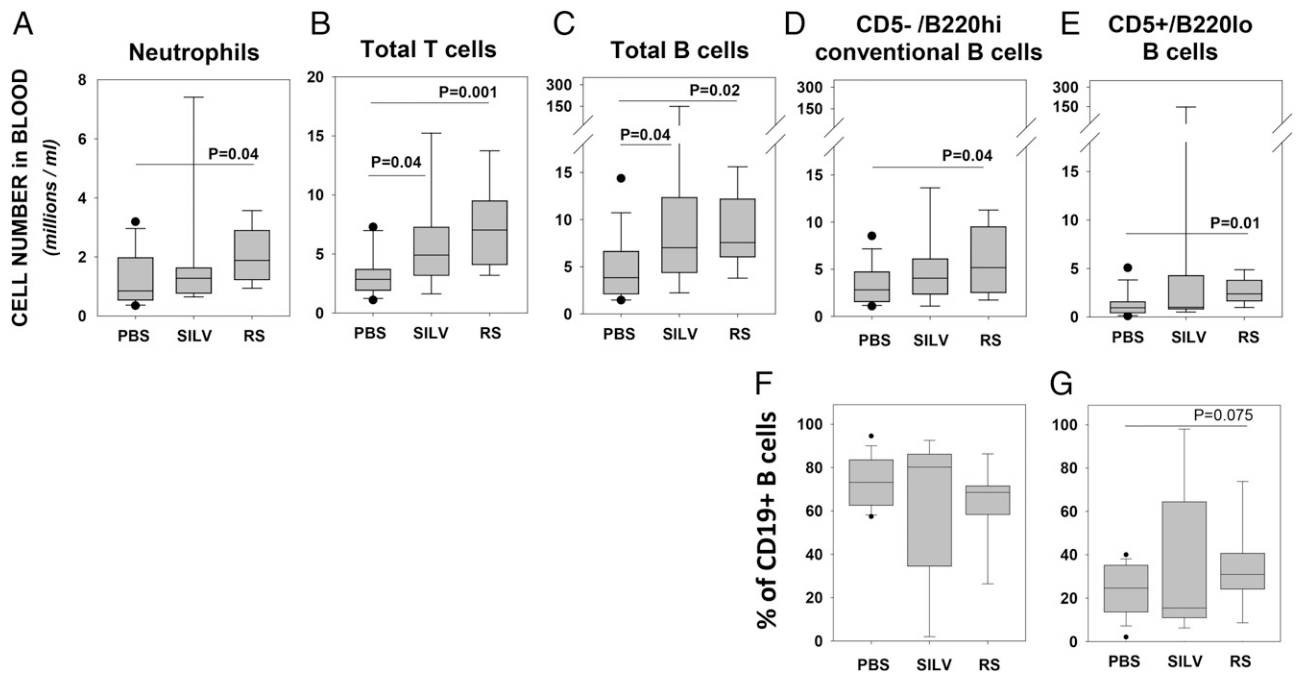

FIGURE 2. ***Coccidioides*** **lung exposure alters blood levels of several leukocyte populations at 6–7 mo of age.**
Shown is the cell frequency (millions/ml) of blood leukocyte populations in mice of each cohort: PBS (n = 14 mice), SILV (*C. posadasii* treated; n = 9), or RS (*C. immitis* treated; n = 8). (**A**–**E**) Boxplots show frequencies of (A) neutrophils, (B) total T cells, (C) total B cells, (D) nonleukemic, normal B cells ($CD5^-/B220^{high}$ and (E) cells with a preleukemic/leukemic phenotype ($CD5^+/B220^{low}$). Note that due to suboptimal monocyte staining in most blood samples taken at this age, insufficient data were available for statistical comparisons of monocyte numbers between cohorts. Nonetheless for two mice of each cohort, satisfactorily stained/gated for monocytes (as in Fig. 1C), the following frequencies were noted (mean ± SD in millions/ml): PBS, 0.24 ± 0.27; SILV, 1.38 ± 1.19; and RS, 0.43 ± 0.04. (**F**) Percent of total $CD19^+$ cells with normal B cell phenotype and (**G**) percent of total $CD19^+$ cells with leukemic phenotype. Differences were determined as statistically significant using a t test, for data with a normal distribution, or a Mann–Whitney rank-sum test for nonparametric data.

intercohort differences. First, the SILV-treated cohort (Fig. 3B) manifested a relatively high incidence of mice (22%) with both rapid B-CLL diagnosis (before 9 mo) and progression to overt B-CLL, as compared with the remaining cohorts (0% of mice with these attributes). Conversely, while RS-treated mice were more uniform in manifesting MBL at 6–8 mo (Figs. 2, 3C), B-CLL diagnosis was typically delayed in this cohort due to waxing and waning frequencies of $CD5^+/B220^{low}$ B cells (e.g., E4-M1, E4-M2, and E16-F2) (Fig. 3C). The latter oscillating pattern was not typical of either the PBS- or SILV-treated cohorts.

Kaplan–Meier incidence plots similarly suggested that certain members of the SILV-treated cohort exhibited more accelerated B-CLL diagnosis (Fig. 4A) and conversion to overt B-CLL (Fig. 4B) than did the other cohorts. However, these differences between the three cohorts were not statistically significant by log-rank statistical analysis. Additional study is needed with larger sample sizes that provide greater statistical power. Likewise, boxplot comparisons of the cohorts for the age of B-CLL manifestation (Fig. 4C) did not show statistically significant variations (p = 0.491). When the age of conversion to overt B-CLL was considered (Fig. 4D), statistically significant intercohort variation was noted (p = 0.025; Kruskal–Wallis one-way ANOVA on ranks). Further pairwise cohort comparisons (Dunn's method) revealed that the age for overt B-CLL diagnosis in SILV-treated mice was significantly earlier than for RS-treated mice (p = 0.03).

Taken together, the above time course analyses revealed unanticipated differences between *C. posadasii* (SILV) and *C. immitis* (RS) arthroconidia in affecting leukemia development. Although not statistically significantly, *C. posadasii* appears to accelerate development in a fraction of TCL1-Tg mice, as compared with controls, and *C. immitis* significantly slows overt B-CLL development when compared with *C. posadasii*–exposed mice.

Comparative B-CLL growth rates within control mice and mice chronically exposed to C. posadasii *(SILV) or* C. immitis *(RS) conidia*

DT analyses were undertaken for insights into the relative growth rate of the emergent B-CLL. Specifically, we wanted to examine 1) whether growth rates of early and late-emerging B-CLL differed; 2) whether leukemic growth rates were affected by *Coccidioides* exposure; and 3) whether leukemias that became overt had intrinsically faster initial growth rates. For these assessments, the frequency (log) of $CD5^+/B220^{low}$ B cells in each leukemic mouse was plotted versus age, beginning from the initiation of linear growth onward through the expansion phase (Fig. 5A–C). DTs were determined from data points for

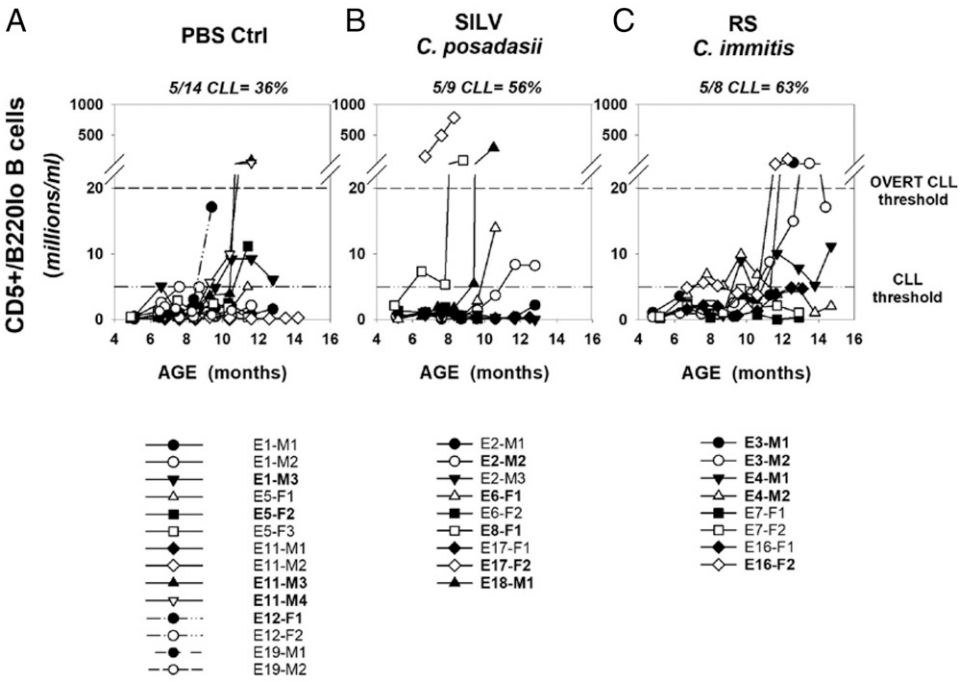

FIGURE 3. Time course for B-CLL emergence within PBS- and *Coccidioides*-exposed TCL1-Tg mice.

(**A**–**C**) Shown are blood frequencies of B cells with the leukemic phenotype ($CD5^+/B220^{low}$) over the lifespan of individual mice chronically exposed to (A) PBS, (B) SILV, or (C) RS. The lower reference line within each graph represents the threshold frequency for B-CLL diagnosis (5 million/ml; see *Materials and Methods* for added criteria). The upper reference line represents the threshold for overt B-CLL diagnosis (20 million $CD5^+/B220^{low}$ B cells/ml). The legend below each graph supplies mouse identification codes; those in bold achieved a B-CLL diagnosis.

linear growth (filled circles), using a Web-based calculator for obtaining DT values (and inversely related growth rates) (5). Not included in these DT assessments were data points representing later "clonal contraction," here defined as declining levels of leukemic cells over time (open circles). Of note, clonal contraction was not apparent in B-CLL of SILV-treated mice, but it was detected in two of five leukemias of the RS-treated cohort (E3-M2 and E4-M2) and one of five leukemias of the PBS-treated control cohorts (E1-M3).

Fig. 5D lists DT for each leukemia in days, together with mouse age at diagnosis (month), and final overt status (+ or −) for each B-CLL. Importantly, we found no statistically significant intercohort differences in B-CLL DT ($p = 0.54$ by Kruskal–Wallis one-way ANOVA on ranks). Furthermore, pooled DT values for all "early" B-CLL were not significantly different from all "late" B-CLL (Fig. 5E). This was the case despite significant differences in the mouse age for leukemia diagnosis (Fig. 5E). However, a difference ($p = 0.07$) was seen when DT values for total "nonovert" B-CLL (light gray bar) were compared with those of total overt B-CLL (dark gray bar) (Fig. 5F, left). This prompted examination of each cohort for DT variation between nonovert and overt subsets (Fig. 5F, right). We found that DT of nonovert B-CLL and overt B-CLL within the RS-treated cohort was significantly different ($p = 0.025$ by a two-sided, unpaired *t* test). Differences of statistical significance were not detected with either the SILV- or PBS-treated cohort.

In summary, when DT analyses are taken together with earlier described characteristics of each B-CLL population, the following insights emerge. Accelerated B-CLL diagnosis in a fraction of SILV-treated mice is not explained by unusually rapid growth rate (shorter DT). Disparity in leukemia DT is evident in all cohorts, but most pronounced in RS-treated mice. Most (three of five) B-CLLs from RS-treated mice are characterized by either clonal contraction and/or slower growth rate (longer DT). In all treatment groups, B-CLL that evolved to overt status displayed comparable DT.

Disease-specific and overall survival time in control and Coccidioides*-exposed TCL1-Tg mice*

During the 15-mo course of this experiment, several mice reached a survival endpoint without manifesting B-CLL. Therefore, Kaplan–Meier survival analyses were performed both for overall survival, representing total mice surviving from death by any cause, and for B-CLL–specific survival. Overall survival curves (Fig. 6A) showed considerable intercohort diversity ($p = 0.003$ by log-rank analysis), largely reflecting the substantially greater survival of RS-treated mice, as compared with the other cohorts ($p = 0.004$ for both RS versus PBS and RS versus SILV, by Holm–Sidak test for pairwise multiple comparisons). Disease (B-CLL)-specific survival curves (Fig. 6B) also manifest intercohort diversity ($p = 0.015$ by log-rank analysis), largely representing differences between RS-treated mice versus SILV-treated and PBS cohorts ($p = 0.03$ and $p = 0.02$, respectively, by the Holm–Sidak test). Although an accelerated demise of SILV-treated mice versus control mice was noted in the disease-specific survival plots, the difference was not statistically significant by log-rank analysis. It is noteworthy that the SILV-treated mice dying at a relatively young age were the same mice exhibiting early breakthrough to overt B-CLL, that is, E17-F2, E8-F1, and E18-M1.

Findings at necropsy suggest that the cause of death in nonleukemic mice varies. When considering those whose death occurred

https://doi.org/10.4049/immunohorizons.2300013

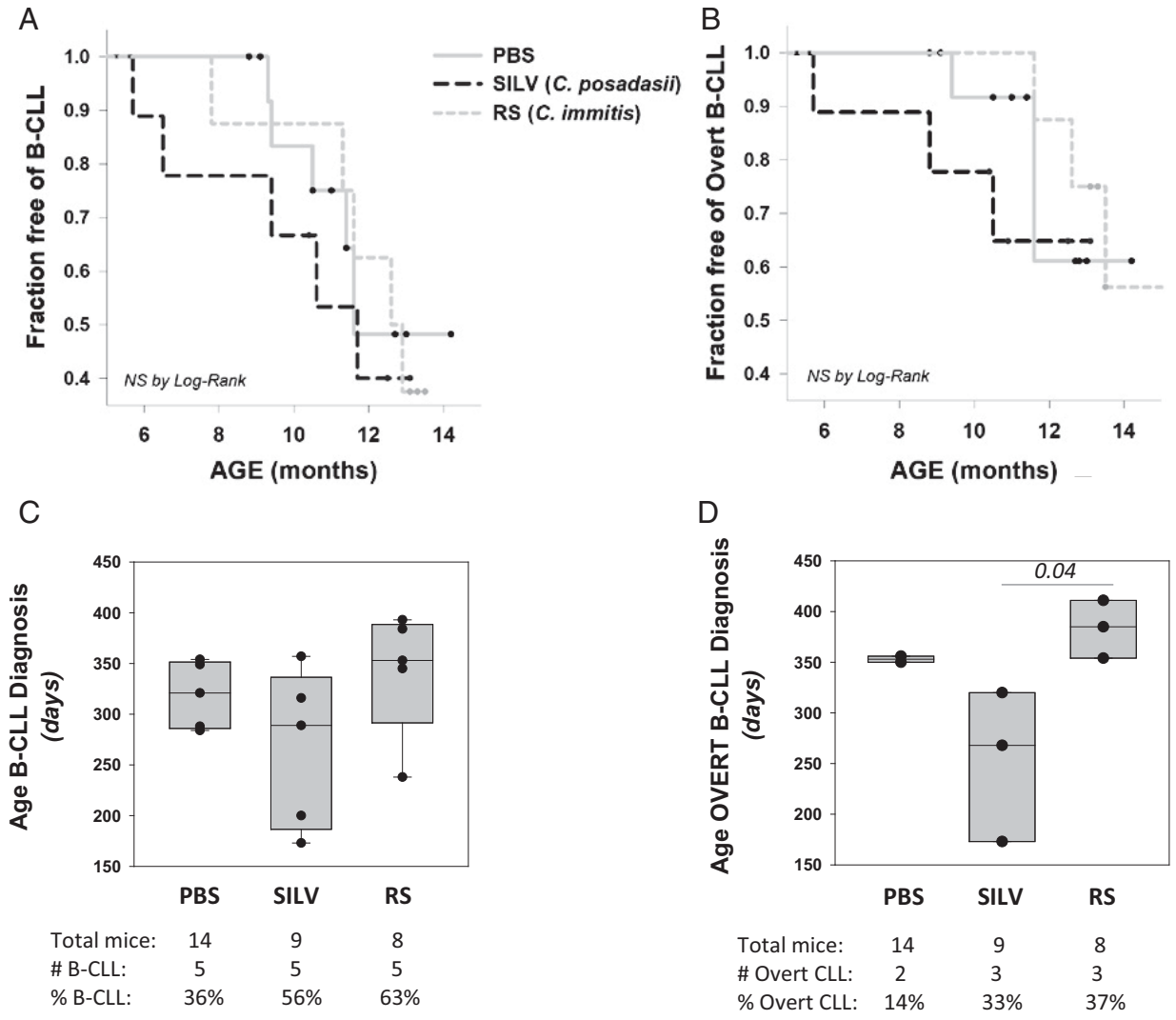

FIGURE 4. Statistical analysis of B-CLL incidence with age.

(**A**) Kaplan–Meier incidence curves, representing the percentage of each cohort that is B-CLL–free over time. Small filled circles stand for censored events, reflecting mouse death without a B-CLL diagnosis. (**B**) Kaplan–Meier incidence curve, representing the percentage of each cohort that is free of overt B-CLL over time. PBS cohort, solid gray; SILV, dashed black; RS, short dash gray. Differences observed in (A) or (B) plots did not reach statistical significance by log-rank analysis. (**C**) Boxplot analysis of pooled data representing age at B-CLL diagnosis within each cohort. Boxes show median levels, with upper and lower quartiles and whiskers representing variability outside the quartiles. Overlaid black circles represent values of individual mice. Statistical analysis (Kruskal–Wallis one-way ANOVA on ranks) showed no significant difference between these groups ($p = 0.491$). (**D**) Boxplot of pooled data representing age at overt B-CLL diagnosis within each cohort. Statistical analysis (as above) revealed a statistically significant difference between these groups ($p = 0.025$). B-CLL cases in the PBS cohort were insufficient to make pairwise comparisons with other cohorts through the unpaired, two-sided *t* test. Nonetheless, ages for overt B-CLL diagnosis in the SILV cohort were statistically different from those in the RS cohort ($p = 0.03$) by the latter analysis.

before 13 mo of age, the following were observed: 1) PBS cohort ($n = 5$): two of five with MBL and either hepatosplenomegaly ($n = 1$) or large thymoma attached to lung ($n = 1$), and three of five without MBL but with splenomegaly with or without hepatomegaly ($n = 2$) or a large, solid lung tumor ($n = 1$); 2) SILV cohort ($n = 2$): all negative for MBL but manifesting either enlarged spleen and notably enlarged thoracic LNs ($n = 1$) or enlarged spleen, abnormal liver, and slightly enlarged thoracic LNs ($n = 1$); 3) RS-treated cohort ($n = 1$) with MBL and hepatosplenomegaly. Importantly, a previous report indicated that 36% of aging Eμ-TCL1–Tg mice develop nonhematological malignancies, particularly histiocytic sarcoma (55). Thus, diminished survival due to a non–B cell malignancy is expected. Nonetheless, the possibility that some TCL1-Tg mice in the current study died of an aggressive B cell lymphoma, without leukemic manifestation, is not excluded.

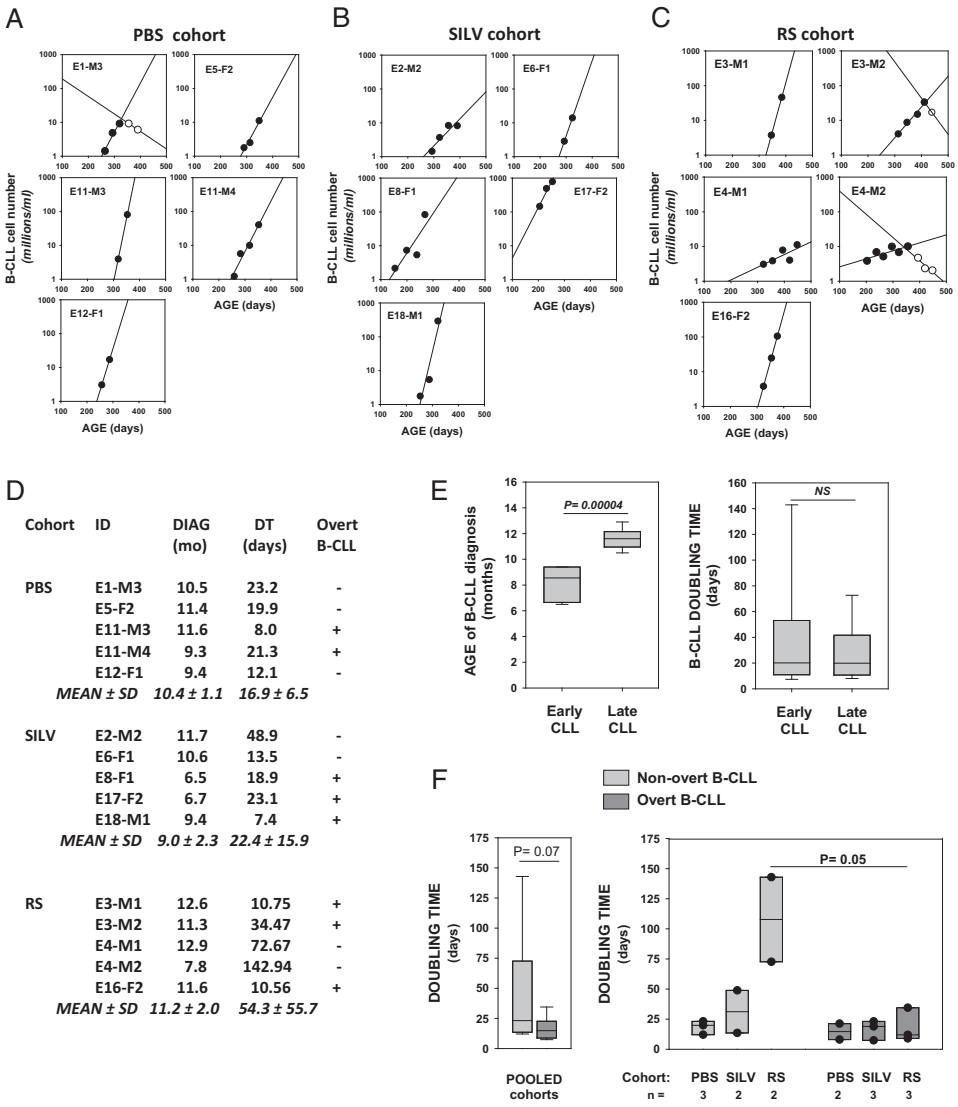

FIGURE 5. Doubling time determinations for B-CLL populations in control and *Coccidioides*-exposed mice.

(**A**–**C**) Linear regression plots showing frequency of $CD5^{+}/B220^{low}$ B cells (log) versus age of mice diagnosed with B-CLL. (A) PBS. (B) SILV. (C) (RS). Lines with filled symbols show the progressive increase in B-CLL numbers over time. The frequencies of $CD5^{+}/B220^{low}$ cells that qualify as preleukemic monoclonal B cell lymphocytosis (MBL = 0.5–5 million/ml) were included in these plots when the latter supplied added confidence in the linear growth curve. Contraction of the leukemic population was seen in certain mice (E1-M3 in PBS cohort; E3-M2 and E4-M2 in RS cohort). Leukemic cell counts during contraction are shown by open symbols; these were not used to compute initial B-CLL doubling time (DT). (**D**) Age of diagnosis (months), DT values (days), and overt status of each B-CLL within the PBS, SILV, and RS cohorts. Calculation of DT was achieved with an online DT calculator based on exponential regression (http://www.doubling-time.com/compute). (**E**) Pooled B-CLLs were categorized as early CLL (n = 6; range, 6.5–9.4 mo) or late CLL (n = 9; range, 10.5–12.9 mo) based on age at diagnosis. By boxplot analysis, the two groups were compared for statistically significant differences in (left) age of B-CLL diagnosis (p = 0.00004 by a two-sided, unpaired t test) and (right) B-CLL DT (not significant). (**F**) Left, Boxplot analysis for DT in total overt versus total nonovert B-CLL populations (p = 0.070 by nonparametric Mann–Whitney rank-sum test). Boxplots for B-CLL DTs in nonovert (light gray bars) versus overt B-CLL (dark gray bars) of each experimental cohort (overlaid filled symbols represent individual mouse values). Median DT for overt B-CLL was consistently low in all cohorts (no statistically significant difference by Kruskal–Wallis one-way ANOVA on ranks). Greater intercohort diversity in DT was seen in nonovert B-CLL, without reaching statistical significance. Nonetheless, within the RS cohort, DT values for nonovert and overt B-CLL were significantly different (p = 0.025 by a one-sided and p = 0.05 by a two-sided, unpaired t test).

In sum, the integration of time course data for B-CLL development and disease-specific survival shows that arthroconidia from two distinct *Coccidioides* species have differing effects on this leukemia. A fraction of mice chronically exposed to *C. posadasii* (SILV) develop B-CLL at earlier ages. These early-appearing B-CLL populations are characterized by

https://doi.org/10.4049/immunohorizons.2300013

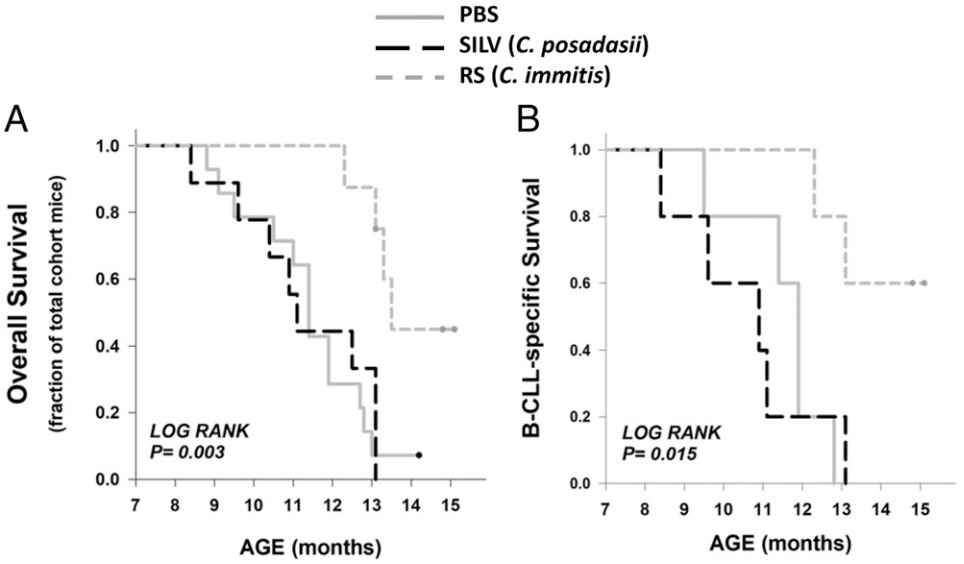

FIGURE 6. Overall and disease-specific survival times in control and *Coccidioides*-exposed TCL1-Tg mice.

(**A**) Kaplan–Meier incidence curves for overall survival (PBS cohort, solid gray; SILV, dashed black; RS, short dash gray). Log rank analysis showed a statistically significant difference within the set of three cohorts ($p = 0.003$). Statistical significance for all pairwise comparisons is as follows (Holm–Sidak test): PBS versus RS ($p = 0.004$), SILV versus RS ($p = 0.004$), and PBS versus SILV ($p = 0.717$). (**B**) Kaplan-Meier incidence curves for disease-specific survival (all mice in this analysis developed B-CLL during the 14-mo course of this study). Log rank analysis showed a statistically significant difference within the set of three cohorts ($p = 0.015$; Holm–Sidak test for pairwise comparisons): PBS versus RS ($p = 0.02$), SILV versus RS ($p = 0.03$), and PBS versus SILV ($p = 0.18$).

rapid growth and accelerated death of mice in which they originated. Conversely, although mice chronically exposed to *C. immitis* (RS) conidia manifest MBL at a faster rate than other cohorts, emergence of B-CLL is not more rapid than in PBS-treated controls. Unexpectedly, *C. immitis* has an attenuating effect on the aggressiveness of most B-CLL and improves mouse survival.

Relationship between B-CLL growth and blood levels of monocytes, neutrophils, and T cells

Prior studies with humans and mice afflicted with B-CLL indicate that monocytes, neutrophils, T cells, and stromal cells play important roles in fostering B-CLL growth (5, 52, 56–59). Because airborne exposure to *Coccidioides* conidia induces vigorous and complex immune responses (60), we postulated that *Coccidioides*-mediated changes in such nonleukemic cells might affect the transformation process and/or the milieu for B-CLL growth. Thus, we compared the frequency of circulating $CD5^+/B220^{low}$ B cells with the frequency of potential accessory cells in monthly blood samples. Frequency data for neutrophils, monocytes, and T cells during the lifespan of individual mice is presented in Supplemental Fig. 2.

Linear regression analyses (Fig. 7) enabled us to assess each cohort (and total experimental mice, or cohort pool) for statistically significant correlations between blood frequencies of $CD5^+/B220^{low}$ B cells and the following differing accessory cell populations.

Neutrophils. As seen in Fig. 7A, a highly significant relationship between neutrophil frequency and levels of circulating $CD5^+/B220^{low}$ B cells (preleukemic and leukemic) was detected in both *Coccidioides*-exposed cohorts ($p = 0.003$ and $p < 0.001$ for SILV and RS, respectively). This was not observed in the PBS control cohort ($p = 0.65$).

Monocytes. Fig. 7B shows that only the SILV-treated cohort exhibited a highly significant link between total monocyte number and $CD5^+/B220^{low}$ B cells ($p < 0.001$). However, a similar trend of borderline statistical significance was seen within the PBS- and RS-treated cohorts ($p = 0.068$ and $p = 0.064$, respectively).

T cells. Fig. 7C shows that T cell frequency was highly linked to the number of circulating $CD5^+/B220^{low}$ B cells, within both the PBS- and SILV-treated cohorts ($p = 0.003$ and $p = 0.004$, respectively). Interestingly, this was not observed in RS-treated mice ($p = 0.857$). Nonetheless, the median frequency of circulating T cells over the lifespan of RS-treated mice (3.2 million T cells/ml blood) was comparable to that of control and SILV-treated cohorts (3.1 and 2.9 million/ml, respectively) (Supplemental Fig. 2D).

Taken together, the above findings suggest that neutrophils play a unique role in fostering B-CLL development in mice exposed to *Coccidioides* conidia of either fungal species. Furthermore, although monocyte levels are associated with B-CLL growth in all mice, this link appears to be most pronounced in mice chronically exposed to *C. posadasii*. Finally, although T cell numbers are statistically linked to B-CLL growth in control and SILV-treated mice, this is not this case for RS-treated mice.

Impact of circulating classical and nonclassical monocyte subsets, M1 and M2, on $CD5^+/B220^{low}$ B cell frequencies

Coccidioides infections are known to elicit both inflammatory and counteracting anti-inflammatory cell populations (60), but the plasticity of the myeloid lineage is little understood (61, 62).

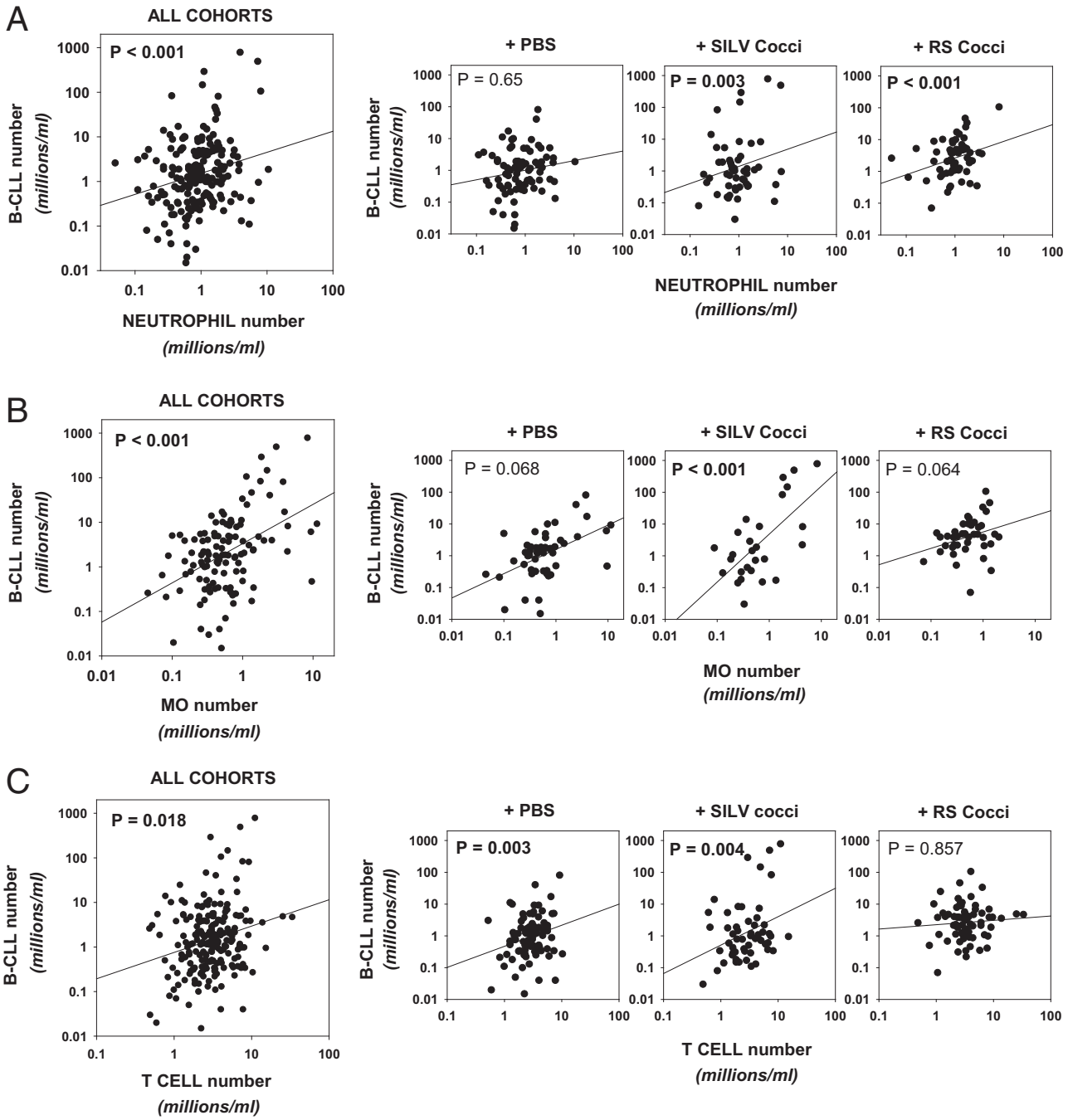

FIGURE 7. CD5$^+$/B220^{low} (preleukemic and leukemic) cell levels in blood are linked to the frequency of other blood leukocyte populations in a cohort-specific manner.

(**A**–**C**) Frequency of CD5$^+$/B220^{low} B cells detected in individual mice at any one blood sampling was plotted against the respective frequency of either (A) neutrophils, (B) monocytes, or (C) T cells. Dot plots and accompanying linear regression lines are shown for pooled mice and mice of each experimental cohort. Values represent data from sequential monthly blood analyses, beginning at 5–6 mo to survival endpoint. In the case of monocytes, fewer mice of each cohort were measured at 5-6 mo. The *p* values for each linear regression analysis are shown, with those reaching statistical significance ($p < 0.05$) in bold.

Because nonclassical (patrolling or anti-inflammatory) monocytes/macrophages (M2 cells) are reported to play a key role in B-CLL development (63, 64), we examined both nonclassical M2 monocytes and classical M1 monocytes within blood samples from the experiment's cohorts. Using correlative analyses, we tested whether B-CLL growth is linked to subpopulation frequency.

Fig. 8A shows the Ly6C-based gating strategy (65–67) used to segregate M1 (Ly6C^{high}) or M2 (Ly6C$^-$) subsets within

https://doi.org/10.4049/immunohorizons.2300013

circulating monocytes ($CD45^+$, $CD11b^{high}$, $Ly6G^-$). Boxplots within Fig. 8B, and accompanying statistics within its legend, show that neither M1 nor M2 monocyte numbers differed significantly in *Coccidioides*-treated mice versus control TCL1-Tg mice. Furthermore, in all cohorts, M2 levels exceeded M1 levels ($p < 0.001$) (Fig. 8B). A high M2/M1 monocyte ratio was earlier associated with the presence of the TCL1 transgene (63); this was confirmed by comparisons of our TCL1-Tg mice with similarly aged, non-Tg C57BL/6 mice (Supplemental Fig. 3). Whereas 12-mo-old normal C57BL/6 mice ($n = 3$) had an M2/M1 ratio of 0.95 ± 0.1 (mean ± SD), the M2/M1 ratios in TCL1-Tg mice were 2.96 ± 1.88, 2.35 ± 0.43, and 2.1 ± 2.45 for the PBS, SILV, and RS cohorts, respectively. The heightened M2/M1 ratio appears to be tumor driven (68, 69).

Linear regression analyses were again employed to examine whether M1 or M2 monocyte frequency was linked to B-CLL numbers in blood (Fig. 8C). Of interest, in all experimental cohorts, a highly significant positive relationship was noted between levels of classical M1 cells and abundance of $CD5^+/B220^{low}$ B cells ($p = 0.002$). However, a significant correlation between nonclassical M2 cells and $CD5^+/B220^{low}$ B cells ($p = 0.047$ and $p = 0.045$, respectively) was observed only in the PBS control- and SILV-treated cohorts.

Table I summarizes the statistically significant relationships noted above. Neutrophil numbers were positively correlated with $CD5^+/B220^{low}$ B cell frequencies only in *Coccidioides*-exposed mice (both SILV and RS). Numbers of $CD5^+/B220^{low}$ B cells and classical M1 monocytes were highly correlated within all three cohorts; however, levels of circulating nonclassical M2 monocytes and total T cells were correlated with levels of preleukemic/leukemic B cells only within the control and SILV-exposed cohorts.

Relationship between $CD5^+/B220^{low}$ B cell frequency in blood and enlargement of peripheral lymphoid tissues

B-CLL clones proliferate within peripheral lymphoid tissues, particularly LNs and spleen (33, 70, 71). These insights prompted us to examine whether the frequency of $CD5^+/B220^{low}$ B cells, in blood taken just prior to a survival endpoint, correlated with hypertrophy of spleen, lung-draining thoracic LNs, and/or non–lung-draining inguinal LNs seen at necropsy. Thoracic LNs were of particular interest given that many are lung draining and hence should be influenced by inhaled microbes (72). Furthermore, thoracic LN enlargement is characteristic of *Coccidioides* infection in humans (73).

The plots in Fig. 9 summarize our findings. For each necropsied mouse, $CD5^+/B220^{low}$ B cell frequency in the last acquired blood sample is plotted against spleen length (Fig. 9A), relative thoracic LN enlargement (Fig. 9B), and relative enlargement of inguinal LNs (Fig. 9C). Linear regression analyses revealed only one statistically significant positive relationship; surprisingly, this is between blood $CD5^+/B220^{low}$ B cell numbers and enlargement of inguinal LNs in RS-treated mice ($p = 0.03$) (Fig. 9C). In SILV-treated mice, positive trend lines toward increased $CD5^+/B220^{low}$ B cell numbers with greater spleen and thoracic LN enlargement are noted, but without statistical significance.

As a further analysis, we compared the relative enlargement of lymphatic tissues in each *Coccidioides*-treated cohort with that seen in the control cohort (Fig. 9). This comparison revealed that RS-treated mice exhibit significantly greater inguinal LN size, as compared with controls ($p = 0.001$ by a two-sided, unpaired t test), whereas SILV-treated mice exhibit a significantly lower inguinal LN size versus control mice ($p = 0.01$). A SILV-associated enlargement of thoracic LNs, as compared with controls, is of borderline statistical significance ($p = 0.09$).

DISCUSSION

In the current study, evidence emerged that chronic microbial infection can impact B-CLL development in complex ways. Repeated lung insult with fixed *Coccidioides* arthroconidia influenced B-CLL development in TCL1-Tg mice, but unexpectedly, in a fungal strain–dependent manner. Following chronic exposure to *C. posadasii* (SILV strain) arthroconidia, a fraction of treated mice manifested accelerated emergence of B-CLL and/or transition into overt B-CLL, and more rapid death as compared with control mice. In contrast, mice exposed to *C. immitis* (RS strain) displayed less aggressive B-CLL development. This was manifested by significantly delayed transition to overt B-CLL, as compared with *C. posadasii*–treated mice, and by slower leukemic cell DTs and significantly prolonged survival, as compared with either PBS- or *C. posadasii*–treated mice. As in earlier studies with TCL1-Tg mice (74–76), each cohort showed considerable variability in the time of B-CLL diagnosis, suggesting that environmental factors influence development, not simply genetics.

The premise that an altered milieu for B-CLL growth contributes to the differing outcomes is supported by statistical correlations found between blood frequencies of $CD5^+B220^{low}$ B cells and potential accessory leukocytes. Neutrophils are strongly linked to $CD5^+B220^{low}$ B cell frequency in mice exposed to either *Coccidioides* species, but not in control mice. Furthermore, whereas M1 monocyte levels are linked to B-CLL growth in all three cohorts, M2 monocyte levels are positively correlated with leukemic cell abundance in *C. posadasii*–exposed and control mice, but not in *C. immitis*–treated mice. Finally, frequencies of blood T cells and $CD5^+/B220^{low}$ B cells are linked in *C. posadasii*–treated and control mice, but not in *C. immitis*–treated mice. The present findings, together with past observations that mouse lungs acutely exposed to *C. posadasii* or *C. immitis* exhibit a distinct inflammatory protein profile (51), support the hypothesis that differences in B-CLL growth within *C. posadasii*– and *C. immitis*–treated TCL1-Tg mice may reflect diverse immunomodulatory effects of these two *Coccidioides* species.

To our knowledge, this study represents the first experimental effort to examine whether fungi, ubiquitous in our environment, affect in vivo B-CLL development. Although diverse geographical settings vary in the predominant fungal populations present (46, 49), *Coccidioides* is a common airborne fungus

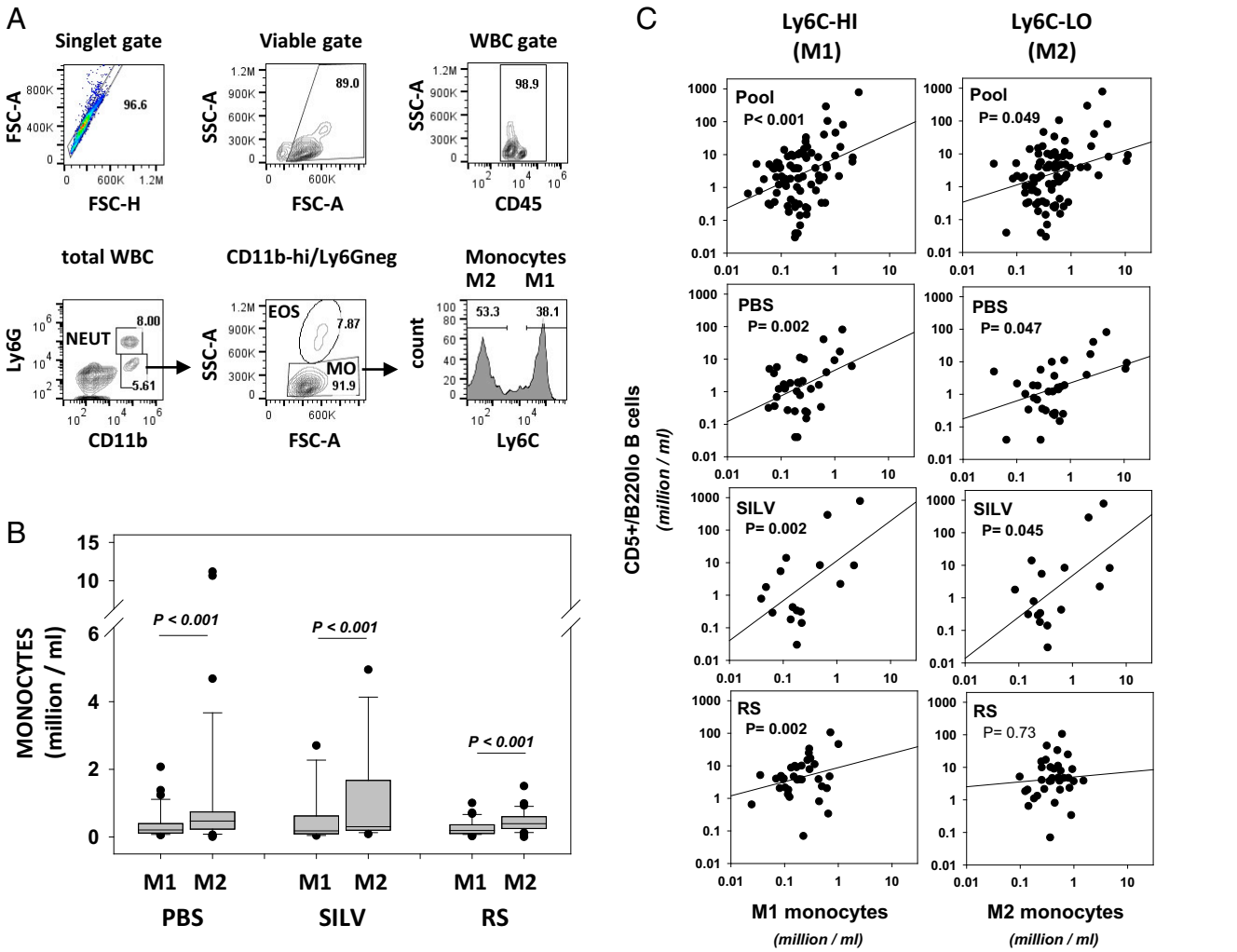

FIGURE 8. Circulating levels of CD5$^+$/B220^{low} B cells are significantly correlated with the frequency of inflammatory (M1) and anti-inflammatory (M2) monocyte subsets in a cohort-specific manner.

(**A**) Gating strategy for segregating classical, inflammatory (M1) monocytes and nonclassical, anti-inflammatory (patrolling) (M2) monocytes. M1 cells represent monocytes (CD45$^+$/Ly6G$^-$/CD11b^{high}/SSC^{low}) that are gated as Ly6C^{high}. M2 cells represent monocytes gated as Ly6C$^-$. Note that monocytes bearing intermediate levels of Ly6C, thought to represent transitional monocytes (64, 65), are not considered. (**B**) Boxplots showing M1 and M2 cell frequencies in pooled monthly bleeds from control TCL1-Tg mice and similar blood samples from SILV-treated and RS-treated cohorts (PBS cohort, n = 13 mice represented with 34 samplings during 6–13 mo; SILV cohort, n = 7 mice, with 16 samplings during 7–12 mo; RS cohort, n = 8 mice, with 35 samplings during 7–14 mo). Note that in this plot closed symbols represent outliers from the boxplot analysis. Comparison of M1 levels (or M2 levels) between the three cohorts by Kruskal–Wallis one-way ANOVA on ranks showed no statistically significant intercohort differences. However, within each cohort the frequency of M2 cells was significantly greater than the corresponding frequency of M1 cells ($p < 0.001$ by paired, two-sided t test). See Supplemental Fig. 3 for comparisons to normal aged C57BL/6 mice. (**C**) Frequency of CD5$^+$B220^{low} B cells is plotted against frequency of M1 cells (left column) or M2 cells (right column). The p values from each linear regression analysis are shown, with those reaching statistical significance ($p < 0.05$) shown in bold. SSC, side scatter.

in arid regions of the United States. Of interest, an earlier clinical report involving Arizona B-CLL patients noted significantly diminished survival in patients infected with *C. posadasii* (77). However, it remains unclear whether the accelerated patient deaths reflected 1) impaired resolution of the fungal infection due to well-recognized leukemia-induced immunosuppression (78–80) and/or 2) enhanced B-CLL growth from stimuli associated with the fungal infection.

The use of formalin-fixed arthroconidia in the current study warrants some discussion. This strategy was deemed necessary due to the uniformly lethal consequences of viable *Coccidioides* infection in mice, particularly in the C57BL/6 strain (81–83). Although not fully mimicking natural infection, this approach yields results unobscured by untoward effects of virulent fungal infection, as in the above-cited clinical study (77). We note that most *Coccidioides*-encoded molecules are shared by the various

https://doi.org/10.4049/immunohorizons.2300013

TABLE I. Summary of statistically significant links between leukemic and accessory cell frequencies in blood

	Neutrophils	M1 Monocytes	M2 Monocytes	T Cells
PBS	–	+	+	+
SILV (*C. posadasii*)	+	+	+	+
RS (*C. immitis*)	+	+	–	–

morphologies exhibited by the fungus (84), and these contribute to inflammatory properties (37). One such shared molecule is β-glucan, a PAMP that engages lectin receptors on immune system cells (85). Dectin-1, a major receptor for fungal β-glucan, is highly expressed on monocytes, macrophages, neutrophils, and dendritic cells (86), present on B cells of C57BL/6 mice (87), and important in *Coccidioides* immunity (88–90). Additionally, both arthroconidia and spherules express TLR9-stimulating CpG DNA, which should stimulate B cells upon arthroconidia internalization (91–93). One issue that remains unresolved is whether the differences noted are representative of all *C. posadasii* and *C. immitis* isolates or are strain specific. This will require further investigation with additional lines from each species.

The observation that only a subset of *C. posadasii*–exposed mice manifests accelerated B-CLL development suggests a stochastic process. One explanation is that chronic *C. posadasii* exposure, beginning at 1 mo of age, facilitated a faster accrual of driver mutations through fostering a milieu for B cell mutagenesis. The latter could be engendered by oxygen and nitrogen species emanating from neutrophils or inflammatory M1 cells (94) and/or heightened expression of mutagenic activation-induced cytosine deaminase (AICDA/AID) in activated B-1 cells. Importantly, AICDA is implicated in B-CLL development (95–99), and molecules elaborated by monocytes, neutrophils, and T cells play critical roles in fostering AICDA expression in normal B cells (100, 101). An alternative explanation for the accelerated emergence of B-CLL within certain SILV-treated mice is the presence of an unusually supportive growth milieu. The latter explanation seems less tenable because the DT of these B-CLLs, while short, was not notably different from many later-appearing B-CLLs.

The *C. immitis* (RS)–treated cohort was the first to uniformly manifest MBL. Thus, it was surprising that B-CLL diagnosis in the latter was often delayed due to waxing and waning levels of circulating $CD5^+B220^{low}$ B cells. Furthermore, B-CLL in RS-treated mice had the slowest DT, and in two of five mice (40%), clonal contraction was apparent with increased age. Similar declines in leukemic cell numbers have been observed in untreated patients and can reflect diminished leukemic cell "birth rate" as well as increased "death rate" (102, 103). A prolonged leukemia DT and clonal contraction are associated with extended survival, as noted in the current study in RS-treated mice. All of the above observations point to suboptimal growth conditions and/or augmented leukemic cell death in RS-treated mice.

Numerous malignancies rely on accessory cells for growth, and this appears particularly so for B-CLL (69). Notably, in this study, we observed that frequency of circulating $CD5^+/B220^{low}$ B cells was highly linked to neutrophil numbers in both *Coccidioides*-exposed cohorts, but not in the control cohort. Other studies have found neutrophil numbers elevated in B-CLL–bearing patients and mice (104–106), but the current study is the first to show a direct role of infectious agents, to our knowledge. This finding is consistent with strong neutrophil-mobilizing properties of *Coccidioides* (37) and evidence that β-glucan–stimulated B cells release neutrophil-attracting chemokines (107). Whether B-CLL cells function similarly to normal B cells upon encounter with fungal β-glucan requires further study. The recent report that neutrophil depletion in TCL1-Tg mice impairs B-CLL growth in spleens (106) emphasizes the B-CLL–promoting function of this myeloid population.

Coccidioides-elicited neutrophils might foster MBL and later B-CLL through the release of neutrophil extracellular traps (NETs) with abundant TLR9-activating DNA (108). Supporting this premise is evidence that NETs directly activate self-reactive memory B cells (109) and enhance survival of B-CLL cells (110); furthermore, neutrophils from B-CLL patients appear particularly effective at releasing NETs (110). Additionally, BAFF and APRIL production from a subset of neutrophils (106) may be relevant. Both TNF family members augment B cell viability, growth, and mutagenic AICDA (100, 101, 111–113). Furthermore, when overexpressed in mice, BAFF and APRIL enhance B-1 cell leukemogenesis (35, 114).

Of additional interest was the observation that numbers of nonclassical M2 monocytes and $CD5^+/B220^{low}$ B cells were significantly linked in *C. posadasii*– and PBS-treated control cohorts, but not in *C. immitis*–treated mice. This finding is consistent with the demonstrated importance of M2 cells for B-CLL development (62, 115) and suggests that M2 cell function is impaired in mice exposed to *C. immitis*.

Notably, in both *Coccidioides*-treated cohorts and the control cohort, the frequency of $CD5^+/B220^{low}$ B cells was significantly linked to classical M1 monocyte levels. This might appear counterintuitive, given strong evidence that nonclassical M2 cells are critical for B-CLL growth (63, 115). Nonetheless, the relevance of M1 cells becomes apparent when stepwise monocyte development is considered. Within bone marrow, premonocyte progenitors differentiate directly into classical M1 cells ($Ly6^{high}$) (116–118). The latter are retained within the bone marrow, via a mechanism involving CXCR4, until inflammatory stimuli prompt their CCL2-mediated release (119, 120). Once in circulation, classical M1 monocytes are relatively short-lived (116). They either are recruited into inflamed tissues, becoming inflammatory M1 monocytes/macrophages (119) (which can sometimes evolve into anti-inflammatory M2 cells [121]), or they differentiate into longer-lived nonclassical M2 monocytes ($Ly6^{low}$) that patrol endothelium (116, 122, 123). Thus, the significant correlation found in the current study between the frequency of blood M1 cells and $CD5^+B220^{low}$ B cells may represent the important precursor role of classical M1 monocytes for the M2 population that directly influences B-CLL development. Consistent with the present link between levels of circulating M1 cells and $CD5^+B220^{low}$ B cells, an earlier report showed that both classical M1 and nonclassical M2 monocytes are elevated in TCL1-Tg mice, as compared with control mice (115).

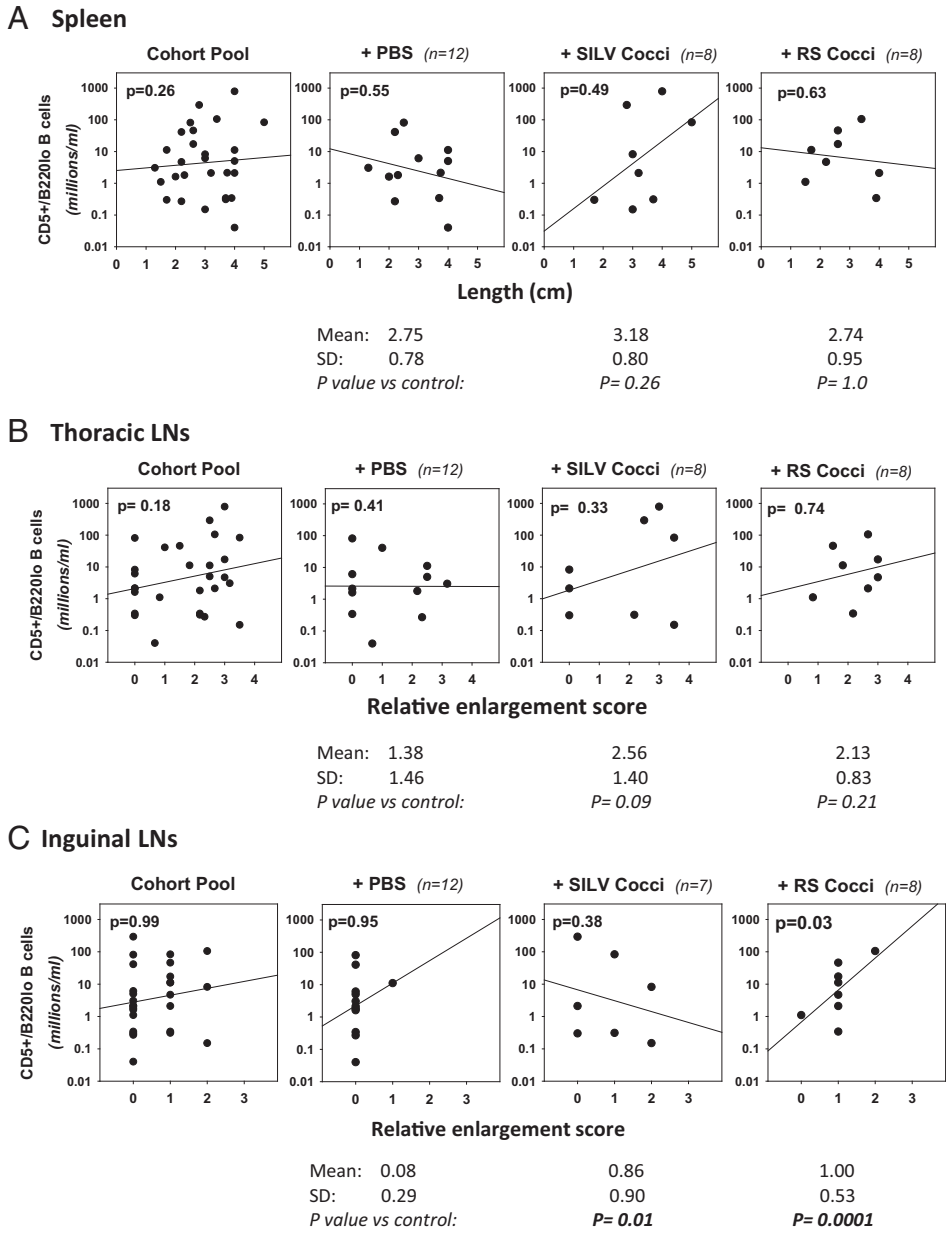

FIGURE 9. Relationship between CD5$^+$/B220^{low} B cell frequency and lymphoid tissue enlargement.

Linear regression analyses were employed for assessing whether the abundance of CD5$^+$/B220^{low} B cells within the last blood sample obtained was statistically linked to enlargement of lymphatic tissues seen at necropsy. Spleen size was determined by assessing length (centimeters). Thoracic and inguinal LN enlargement was assessed subjectively and scored, as described in *Materials and Methods*. (**A**) Spleen. Shown are dot plots and linear regression lines comparing CD5$^+$/B220^{low} B cell number and spleen size (centimeter length) (left to right) within the cohort pool, and control, SILV-treated, or RS-treated individual cohorts. No statistically significant relationship between these parameters was noted in any cohort. Values below each cohort plot represent spleen size in centimeters (mean ± SD) as well as *p* values from a statistical comparison of spleen size within the control cohort and each *Coccidioides*-treated cohort, employing either a parametric *t* test or nonparametric Mann–Whitney rank-sum test. No significant difference from control mice was noted. (**B**) Thoracic LNs. A similar analysis with thoracic LNs revealed no statistically significant relationship between CD5$^+$/B220^{low} B cell numbers and relative thoracic LN enlargement in any cohort. However, when thoracic LN size within the control cohort was compared with that of the *Coccidioides*-treated cohorts, the greater size within SILV-treated mice (enlargement score of 2.56 versus 1.38 in control mice) approached statistical significance ($p = 0.09$). (**C**) Inguinal LNs. By linear regression analysis, a statistically significant relationship was noted between CD5$^+$/B220^{low} B cell numbers and relative inguinal LN enlargement in RS-treated mice ($p = 0.03$), but not other cohorts. Values below each plot reveal that inguinal LN enlargement scores within both the SILV-treated and the RS-treated cohorts were statistically greater than those in the control cohort ($p = 0.01$ and $p = 0.0001$, respectively). Of note, necropsy was not performed in 2 of 14 total PBS-treated mice (E12-F1 and E12-F2) and in 1 of 8 total SILV-treated mice (E6-F1) due to body deterioration after unanticipated death.

https://doi.org/10.4049/immunohorizons.2300013

In addition, frequencies of both the M1 and M2 populations were elevated in blood of B-CLL patients versus control individuals (57). Recently, a clinical study found that an inflammatory blood monocyte profile was strongly associated with the B-CLL precursor state, MBL, but less apparent as patients progressed to frank B-CLL (124). Thus, the proportion of these subpopulations may change as leukemia progresses.

Extensive studies in both humans and mice indicate that circulating levels of both $CD8^+$ and $CD4^+$ T cells rise in B-CLL (reviewed in Ref. 125), yet there is considerable ambiguity concerning whether T cells have a major growth-fostering role (115, 125, 126). Genetic ablation of CD40-L fails to affect B-CLL development, suggesting that CD40 signals are not necessary in this setting (115, 126). Nonetheless, activated T cells could positively influence B-CLL progression through synthesis of growth-promoting cytokines (115) or, alternatively, immunosuppressive IL-10 (115, 127, 128). Although $CD8^+$ T cells are expanded in B-CLL (125, 129–131), these potential tumor-suppressive cells are dysfunctional, and leukemia cell–elaborated IL-10 is at least in part responsible (127).

Although speculative, it warrants considering why the *C. immitis*–treated cohort was unique in not manifesting a link between circulating T cell and $CD5^+/B220^{low}$ B cell frequencies. Of potential relevance is the past observation that IL-10 levels were significantly lower within lungs of normal mice acutely exposed to *C. immitis* versus *C. posadasii* arthroconidia (51). Possibly, *C. immitis* elicits mechanisms to dampen IL-10 synthesis and these mitigate the $CD8^+$ dysfunction typical of B-CLL. This hypothesis is consistent with the restrained B-CLL growth within *C. immitis*–treated mice as well as the absent correlation between frequencies of $CD5^+B220^{low}$ B cells and T cells. It is also in line with evidence that inguinal LNs, rather than lung-draining thoracic LNs, are significantly enlarged in *C. immitis*–treated mice. Possibly, cytotoxic $CD8^+$ T cells are more functional within the latter's lung-draining thoracic LNs, curtailing B-CLL growth within this site. Further study is needed to test the validity of this hypothesis.

Chronic infections, microbiota, and inflammation are implicated in cancers, including hematological malignancies (132–138). Nonetheless, microbiome studies show that certain microbes are anti-inflammatory and counteract a variety of immune-related disorders (reviewed in Ref. 139) and/or are linked to better survival during malignancy (135). Expanded characterization of the infectious agents able to amplify or suppress B-CLL development should lead to enhanced clinical intervention and improved survival of our aging population.

DISCLOSURES

The authors have no financial conflicts of interest.

ACKNOWLEDGMENTS

We thank Dr. Carlo Croce for permitting access to mice with the Eu-TCL1 transgene, developed in his laboratory; Drs. Nicholas Chiorazzi and Xiao J. Yan for supplying breeding pairs of Eu-TCL1–Tg mice on the C57BL/6 background; Dr. Narendiran Rajasekaran for providing access to his laboratory's CytoFLEX flow cytometer; Dr. Sophia Carvalho for providing training in the use of the CytoFLEX flow cytometer; Dr. Fernando Monroy for sharing his laboratory for the performance of the current study's B-CLL analyses; Dr. Marley C. Caballero for supplying training in the intranasal delivery of arthroconidia; Kathleen Freel for dedicated management of the Biological Sciences Annex animal use facility and help in monitoring animals under study; and Drs. Kimberley Cohen and Dale DeNardo for veterinary assistance.

REFERENCES

1. Scarfò, L., and P. Ghia. 2016. What does it mean I have a monoclonal B-cell lymphocytosis?: recent insights and new challenges. *Semin. Oncol.* 43: 201–208.
2. Kolijn, P. M., F. S. Hosnijeh, F. Späth, P. J. Hengeveld, A. Agathangelidis, M. Saleh, D. Casabonne, Y. Benavente, M. Jerkeman, A. Agudo, et al. 2022. High-risk subtypes of chronic lymphocytic leukemia are detectable as early as 16 years prior to diagnosis. *Blood* 139: 1557–1563.
3. Messmer, B. T., E. Albesiano, D. G. Efremov, F. Ghiotto, S. L. Allen, J. Kolitz, R. Foa, R. N. Damle, F. Fais, D. Messmer, et al. 2004. Multiple distinct sets of stereotyped antigen receptors indicate a role for antigen in promoting chronic lymphocytic leukemia. *J. Exp. Med.* 200: 519–525.
4. Herishanu, Y., B. Z. Katz, A. Lipsky, and A. Wiestner. 2013. Biology of chronic lymphocytic leukemia in different microenvironments: clinical and therapeutic implications. *Hematol. Oncol. Clin. North Am.* 27: 173–206.
5. Mongini, P. K., R. Gupta, E. Boyle, J. Nieto, H. Lee, J. Stein, J. Bandovic, T. Stankovic, J. Barrientos, J. E. Kolitz, et al. 2015. TLR-9 and IL-15 synergy promotes the in vitro clonal expansion of chronic lymphocytic leukemia B cells. *J. Immunol.* 195: 901–923.
6. Gupta, R., X. J. Yan, J. Barrientos, J. E. Kolitz, S. L. Allen, K. Rai, N. Chiorazzi, and P. K. A. Mongini. 2018. Mechanistic insights into CpG DNA and IL-15 synergy in promoting B cell chronic lymphocytic leukemia clonal expansion. *J. Immunol.* 201: 1570–1585.
7. Landau, D. A., S. L. Carter, P. Stojanov, A. McKenna, K. Stevenson, M. S. Lawrence, C. Sougnez, C. Stewart, A. Sivachenko, L. Wang, et al. 2013. Evolution and impact of subclonal mutations in chronic lymphocytic leukemia. *Cell* 152: 714–726.
8. Zaborsky, N., F. J. Gassner, J. P. Höpner, M. Schubert, D. Hebenstreit, R. Stark, D. Asslaber, M. Steiner, R. Geisberger, R. Greil, and A. Egle. 2019. Exome sequencing of the TCL1 mouse model for CLL reveals genetic heterogeneity and dynamics during disease development. *Leukemia* 33: 957–968.
9. Jiménez, I., B. Tazón-Vega, P. Abrisqueta, J. C. Nieto, S. Bobillo, C. Palacio-García, J. Carabia, R. Valdés-Mas, M. Munuera, L. Puigdefàbregas, et al. 2021. Immunological and genetic kinetics from diagnosis to clinical progression in chronic lymphocytic leukemia. *Biomark. Res.* 9: 37.
10. Cole, L. E., Y. Yang, K. L. Elkins, E. T. Fernandez, N. Qureshi, M. J. Shlomchik, L. A. Herzenberg, L. A. Herzenberg, and S. N. Vogel. 2009. Antigen-specific B-1a antibodies induced by *Francisella tularensis* LPS provide long-term protection against *F. tularensis* LVS challenge. *Proc. Natl. Acad. Sci. USA* 106: 4343–4348.
11. Choi, Y. S., and N. Baumgarth. 2008. Dual role for B-1a cells in immunity to influenza virus infection. *J. Exp. Med.* 205: 3053–3064.
12. Subramaniam, K. S., K. Datta, E. Quintero, C. Manix, M. S. Marks, and L. A. Pirofski. 2010. The absence of serum IgM enhances the susceptibility of mice to pulmonary challenge with *Cryptococcus neoformans*. *J. Immunol.* 184: 5755–5767.

13. Smith, F. L., and N. Baumgarth. 2019. B-1 cell responses to infections. *Curr. Opin. Immunol.* 57: 23–31.
14. Silverman, G. J. 2015. Protective natural autoantibodies to apoptotic cells: evidence of convergent selection of recurrent innate-like clones. *Ann. N. Y. Acad. Sci.* 1362: 164–175.
15. Baumgarth, N. 2016. B-1 cell heterogeneity and the regulation of natural and antigen-induced IgM production. *Front. Immunol.* 7: 324.
16. Baumgarth, N. 2011. The double life of a B-1 cell: self-reactivity selects for protective effector functions. *Nat. Rev. Immunol.* 11: 34–46.
17. Cunningham, A. F., A. Flores-Langarica, S. Bobat, C. C. Dominguez Medina, C. N. Cook, E. A. Ross, C. Lopez-Macias, and I. R. Henderson. 2014. B1b cells recognize protective antigens after natural infection and vaccination. *Front. Immunol.* 5: 535.
18. Hoogeboom, R., K. P. van Kessel, F. Hochstenbach, T. A. Wormhoudt, R. J. Reinten, K. Wagner, A. P. Kater, J. E. Guikema, R. J. Bende, and C. J. van Noesel. 2013. A mutated B cell chronic lymphocytic leukemia subset that recognizes and responds to fungi. *J. Exp. Med.* 210: 59–70.
19. Hervé, M., K. Xu, Y. S. Ng, H. Wardemann, E. Albesiano, B. T. Messmer, N. Chiorazzi, and E. Meffre. 2005. Unmutated and mutated chronic lymphocytic leukemias derive from self-reactive B cell precursors despite expressing different antibody reactivity. *J. Clin. Invest.* 115: 1636–1643.
20. Agathangelidis, A., N. Darzentas, A. Hadzidimitriou, X. Brochet, F. Murray, X. J. Yan, Z. Davis, E. J. van Gastel-Mol, C. Tresoldi, C. C. Chu, et al. 2012. Stereotyped B-cell receptors in one-third of chronic lymphocytic leukemia: a molecular classification with implications for targeted therapies. *Blood* 119: 4467–4475.
21. Yan, X. J., E. Albesiano, N. Zanesi, S. Yancopoulos, A. Sawyer, E. Romano, A. Petlickovski, D. G. Efremov, C. M. Croce, and N. Chiorazzi. 2006. B cell receptors in TCL1 transgenic mice resemble those of aggressive, treatment-resistant human chronic lymphocytic leukemia. *Proc. Natl. Acad. Sci. USA* 103: 11713–11718.
22. Zhang, S., and T. J. Kipps. 2014. The pathogenesis of chronic lymphocytic leukemia. *Annu. Rev. Pathol.* 9: 103–118.
23. Ghiotto, F., F. Fais, A. Valetto, E. Albesiano, S. Hashimoto, M. Dono, H. Ikematsu, S. L. Allen, J. Kolitz, K. R. Rai, et al. 2004. Remarkably similar antigen receptors among a subset of patients with chronic lymphocytic leukemia. *J. Clin. Invest.* 113: 1008–1016.
24. Lanemo Myhrinder, A., E. Hellqvist, E. Sidorova, A. Söderberg, H. Baxendale, C. Dahle, K. Willander, G. Tobin, E. Bäckman, O. Söderberg, et al. 2008. A new perspective: molecular motifs on oxidized LDL, apoptotic cells, and bacteria are targets for chronic lymphocytic leukemia antibodies. *Blood* 111: 3838–3848.
25. Hatzi, K., R. Catera, C. Moreno Atanasio, V. A. Fischetti, S. L. Allen, J. E. Kolitz, K. R. Rai, C. C. Chu, and N. Chiorazzi. 2016. Chronic lymphocytic leukemia immunoglobulins display bacterial reactivity that converges and diverges from auto-/poly-reactivity and IGHV mutation status. *Clin. Immunol.* 172: 44–51.
26. Steininger, C., G. F. Widhopf II, E. M. Ghia, C. S. Morello, K. Vanura, R. Sanders, D. Spector, D. Guiney, U. Jäger, and T. J. Kipps. 2012. Recombinant antibodies encoded by IGHV1-69 react with pUL32, a phosphoprotein of cytomegalovirus and B-cell superantigen. *Blood* 119: 2293–2301.
27. Landgren, O., J. S. Rapkin, N. E. Caporaso, L. Mellemkjaer, G. Gridley, L. R. Goldin, and E. A. Engels. 2007. Respiratory tract infections and subsequent risk of chronic lymphocytic leukemia. *Blood* 109: 2198–2201.
28. Kostareli, E., A. Hadzidimitriou, N. Stavroyianni, N. Darzentas, A. Athanasiadou, M. Gounari, V. Bikos, A. Agathagelidis, T. Touloumenidou, I. Zorbas, et al. 2009. Molecular evidence for EBV and CMV persistence in a subset of patients with chronic lymphocytic leukemia expressing stereotyped IGHV4-34 B-cell receptors. *Leukemia* 23: 919–924.
29. Kirby, A. C., M. C. Coles, and P. M. Kaye. 2009. Alveolar macrophages transport pathogens to lung draining lymph nodes. *J. Immunol.* 183: 1983–1989.
30. Dadashian, E. L., E. M. McAuley, D. Liu, A. L. Shaffer III, R. M. Young, J. R. Iyer, M. J. Kruhlak, L. M. Staudt, A. Wiestner, and S. E. M. Herman. 2019. TLR signaling is activated in lymph node-resident CLL cells and is only partially inhibited by ibrutinib. *Cancer Res.* 79: 360–371.
31. Muzio, M., E. Fonte, and F. Caligaris-Cappio. 2012. Toll-like receptors in chronic lymphocytic leukemia. *Mediterr. J. Hematol. Infect. Dis.* 4: e2012055.
32. Rozková, D., L. Novotná, R. Pytlík, I. Hochová, T. Kozák, J. Bartunková, and R. Spísek. 2010. Toll-like receptors on B-CLL cells: expression and functional consequences of their stimulation. *Int. J. Cancer* 126: 1132–1143.
33. Bichi, R., S. A. Shinton, E. S. Martin, A. Koval, G. A. Calin, R. Cesari, G. Russo, R. R. Hardy, and C. M. Croce. 2002. Human chronic lymphocytic leukemia modeled in mouse by targeted TCL1 expression. *Proc. Natl. Acad. Sci. USA* 99: 6955–6960.
34. Simonetti, G., M. T. Bertilaccio, P. Ghia, and U. Klein. 2014. Mouse models in the study of chronic lymphocytic leukemia pathogenesis and therapy. *Blood* 124: 1010–1019.
35. Enzler, T., A. P. Kater, W. Zhang, G. F. Widhopf II, H. Y. Chuang, J. Lee, E. Avery, C. M. Croce, M. Karin, and T. J. Kipps. 2009. Chronic lymphocytic leukemia of Emu-TCL1 transgenic mice undergoes rapid cell turnover that can be offset by extrinsic CD257 to accelerate disease progression. *Blood* 114: 4469–4476.
36. Johnson, L., E. M. Gaab, J. Sanchez, P. Q. Bui, C. J. Nobile, K. K. Hoyer, M. W. Peterson, and D. M. Ojcius. 2014. Valley fever: danger lurking in a dust cloud. *Microbes Infect.* 16: 591–600.
37. Van Dyke, M. C. C., G. R. Thompson, J. N. Galgiani, and B. M. Barker. 2019. The rise of *Coccidioides*: forces against the dust devil unleashed. *Front. Immunol.* 10: 2188.
38. Lewis, E. R., J. R. Bowers, and B. M. Barker. 2015. Dust devil: the life and times of the fungus that causes Valley fever. *PLoS Pathog.* 11: e1004762.
39. Beaman, L. V., D. Pappagianis, and E. Benjamini. 1979. Mechanisms of resistance to infection with *Coccidioides immitis* in mice. *Infect. Immun.* 23: 681–685.
40. Hung, C. Y., A. Gonzalez, M. Wüthrich, B. S. Klein, and G. T. Cole. 2011. Vaccine immunity to coccidioidomycosis occurs by early activation of three signal pathways of T helper cell response (Th1, Th2, and Th17). *Infect. Immun.* 79: 4511–4522.
41. Li, L., S. M. Dial, M. Schmelz, M. A. Rennels, and N. M. Ampel. 2005. Cellular immune suppressor activity resides in lymphocyte cell clusters adjacent to granulomata in human coccidioidomycosis. *Infect. Immun.* 73: 3923–3928.
42. Shubitz, L. F., S. M. Dial, R. Perrill, R. Casement, and J. N. Galgiani. 2008. Vaccine-induced cellular immune responses differ from innate responses in susceptible and resistant strains of mice infected with *Coccidioides posadasii*. *Infect. Immun.* 76: 5553–5564.
43. Candando, K. M., J. M. Lykken, and T. F. Tedder. 2014. B10 cell regulation of health and disease. *Immunol. Rev.* 259: 259–272.
44. DiLillo, D. J., J. B. Weinberg, A. Yoshizaki, M. Horikawa, J. M. Bryant, Y. Iwata, T. Matsushita, K. M. Matta, Y. Chen, G. M. Venturi, et al. 2013. Chronic lymphocytic leukemia and regulatory B cells share IL-10 competence and immunosuppressive function. *Leukemia* 27: 170–182.
45. McCotter, O. Z., K. Benedict, D. M. Engelthaler, K. Komatsu, K. D. Lucas, J. C. Mohle-Boetani, H. Oltean, D. Vugia, T. M. Chiller, G. L. Sondermeyer Cooksey, et al. 2019. Update on the Epidemiology of coccidioidomycosis in the United States. *Med. Mycol.* 57(Suppl. 1): S30–S40.
46. Sharpton, T. J., J. E. Stajich, S. D. Rounsley, M. J. Gardner, J. R. Wortman, V. S. Jordar, R. Maiti, C. D. Kodira, D. E. Neafsey, Q. Zeng, et al. 2009. Comparative genomic analyses of the human fungal pathogens *Coccidioides* and their relatives. *Genome Res.* 19: 1722–1731.
47. Thompson III, G. R. 2011. Pulmonary coccidioidomycosis. *Semin. Respir. Crit. Care Med.* 32: 754–763.

48. Valdivia, L., D. Nix, M. Wright, E. Lindberg, T. Fagan, D. Lieberman, T. Stoffer, N. M. Ampel, and J. N. Galgiani. 2006. Coccidioidomycosis as a common cause of community-acquired pneumonia. *Emerg. Infect. Dis.* 12: 958–962.
49. Kollath, D. R., K. J. Miller, and B. M. Barker. 2019. The mysterious desert dwellers: *Coccidioides immitis* and *Coccidioides posadasii*, causative fungal agents of coccidioidomycosis. *Virulence* 10: 222–233.
50. Fisher, M. C., G. L. Koenig, T. J. White, G. San-Blas, R. Negroni, I. G. Alvarez, B. Wanke, and J. W. Taylor. 2001. Biogeographic range expansion into South America by *Coccidioides immitis* mirrors New World patterns of human migration. *Proc. Natl. Acad. Sci. USA* 98: 4558–4562.
51. Lewis, E. R., V. R. David, A. L. Doyle, K. Rajabi, J. A. Kiefer, P. Pirrotte, and B. M. Barker. 2015. Differences in host innate responses among *Coccidioides* isolates in a murine model of pulmonary coccidioidomycosis. *Eukaryot. Cell* 14: 1043–1053.
52. Bresin, A., L. D'Abundo, M. G. Narducci, M. T. Fiorenza, C. M. Croce, M. Negrini, and G. Russo. 2016. TCL1 transgenic mouse model as a tool for the study of therapeutic targets and microenvironment in human B-cell chronic lymphocytic leukemia. *Cell Death Dis.* 7: e2071.
53. de Melo Teixeira, M., J. E. Stajich, J. W. Sahl, G. R. Thompson, R. B. Brem, C. A. Dubin, A. V. Blackmon, H. L. Mead, P. Keim, and B. M. Barker. 2022. A chromosomal-level reference genome of the widely utilized *Coccidioides posadasii* laboratory strain "Silveira". *G3 (Bethesda)* 12: jkac031.
54. Mead, H. L., M. C. C. Van Dyke, and B. M. Barker. 2020. Proper care and feeding of *Coccidioides*: a laboratorian's guide to cultivating the dimorphic stages of *C. immitis* and *C. posadasii*. *Curr. Protoc. Microbiol.* 58: e113.
55. Zanesi, N., R. Aqeilan, A. Drusco, M. Kaou, C. Sevignani, S. Costinean, L. Bortesi, G. La Rocca, P. Koldovsky, S. Volinia, et al. 2006. Effect of rapamycin on mouse chronic lymphocytic leukemia and the development of nonhematopoietic malignancies in Emu-TCL1 transgenic mice. *Cancer Res.* 66: 915–920.
56. Burger, J. A. 2011. Nurture versus nature: the microenvironment in chronic lymphocytic leukemia. *Hematology (Am. Soc. Hematol. Educ. Program)* 2011: 96–103.
57. Maffei, R., J. Bulgarelli, S. Fiorcari, L. Bertoncelli, S. Martinelli, C. Guarnotta, I. Castelli, S. Deaglio, G. Debbia, S. De Biasi, et al. 2013. The monocytic population in chronic lymphocytic leukemia shows altered composition and deregulation of genes involved in phagocytosis and inflammation. *Haematologica* 98: 1115–1123.
58. Wachowska, M., A. Wojciechowska, and A. Muchowicz. 2021. The role of neutrophils in the pathogenesis of chronic lymphocytic leukemia. *Int. J. Mol. Sci.* 23: 365.
59. Galletti, G., C. Scielzo, F. Barbaglio, T. V. Rodriguez, M. Riba, D. Lazarevic, D. Cittaro, G. Simonetti, P. Ranghetti, L. Scarfò, et al. 2016. Targeting macrophages sensitizes chronic lymphocytic leukemia to apoptosis and inhibits disease progression. *Cell Rep.* 14: 1748–1760.
60. Donovan, F. M., L. Shubitz, D. Powell, M. Orbach, J. Frelinger, and J. N. Galgiani. 2019. Early events in coccidioidomycosis. *Clin. Microbiol. Rev.* 33: e00112-19.
61. Diep, A. L., S. Tejeda-Garibay, N. Miranda, and K. K. Hoyer. 2021. Macrophage and dendritic cell activation and polarization in response to *Coccidioidesposadasii* infection. *J. Fungi (Basel)* 7: 630.
62. Diep, A. L., and K. K. Hoyer. 2020. Host response to *Coccidioides* infection: fungal immunity. *Front. Cell. Infect. Microbiol.* 10: 581101.
63. Hanna, B. S., F. McClanahan, H. Yazdanparast, N. Zaborsky, V. Kalter, P. M. Rößner, A. Benner, C. Dürr, A. Egle, J. G. Gribben, et al. 2016. Depletion of CLL-associated patrolling monocytes and macrophages controls disease development and repairs immune dysfunction in vivo. *Leukemia* 30: 570–579.
64. Mesaros, O., L. Jimbu, A. Neaga, C. Popescu, I. Berceanu, C. Tomuleasa, B. Fetica, and M. Zdrenghea. 2020. Macrophage polarization in chronic lymphocytic leukemia: nurse-like cells are the caretakers of leukemic cells. *Biomedicines* 8: 516.
65. Polletti, S., and G. Natoli. 2017. Understanding spontaneous conversion: the case of the Ly6C$^-$ monocyte. *Immunity* 46: 764–766.
66. Ginhoux, F., and S. Jung. 2014. Monocytes and macrophages: developmental pathways and tissue homeostasis. *Nat. Rev. Immunol.* 14: 392–404.
67. Ingersoll, M. A., R. Spanbroek, C. Lottaz, E. L. Gautier, M. Frankenberger, R. Hoffmann, R. Lang, M. Haniffa, M. Collin, F. Tacke, et al. 2010. Comparison of gene expression profiles between human and mouse monocyte subsets. *Blood* 115: e10–e19.
68. Audrito, V., S. Serra, D. Brusa, F. Mazzola, F. Arruga, T. Vaisitti, M. Coscia, R. Maffei, D. Rossi, T. Wang, et al. 2015. Extracellular nicotinamide phosphoribosyltransferase (NAMPT) promotes M2 macrophage polarization in chronic lymphocytic leukemia. *Blood* 125: 111–123.
69. Fiorcari, S., R. Maffei, C. G. Atene, L. Potenza, M. Luppi, and R. Marasca. 2021. Nurse-like cells and chronic lymphocytic leukemia B cells: a mutualistic crosstalk inside tissue microenvironments. *Cells* 10: 217.
70. Herishanu, Y., P. Pérez-Galán, D. Liu, A. Biancotto, S. Pittaluga, B. Vire, F. Gibellini, N. Njuguna, E. Lee, L. Stennett, et al. 2011. The lymph node microenvironment promotes B-cell receptor signaling, NF-κB activation, and tumor proliferation in chronic lymphocytic leukemia. *Blood* 117: 563–574.
71. Chen, S. S., F. Batliwalla, N. E. Holodick, X. J. Yan, S. Yancopoulos, C. M. Croce, T. L. Rothstein, and N. Chiorazzi. 2013. Autoantigen can promote progression to a more aggressive TCL1 leukemia by selecting variants with enhanced B-cell receptor signaling. *Proc. Natl. Acad. Sci. USA* 110: E1500–E1507.
72. Chackerian, A. A., J. M. Alt, T. V. Perera, C. C. Dascher, and S. M. Behar. 2002. Dissemination of *Mycobacterium tuberculosis* is influenced by host factors and precedes the initiation of T-cell immunity. *Infect. Immun.* 70: 4501–4509.
73. Nin, C. S., V. V. de Souza, R. H. do Amaral, R. Schuhmacher Neto, G. R. Alves, E. Marchiori, K. L. Irion, F. Balbinot, G. S. Meirelles, P. Santana, et al. 2016. Thoracic lymphadenopathy in benign diseases: a state of the art review. *Respir. Med.* 112: 10–17.
74. Iacovelli, S., E. Hug, S. Bennardo, M. Duehren-von Minden, S. Gobessi, A. Rinaldi, M. Suljagic, D. Bilbao, G. Bolasco, J. Eckl-Dorna, et al. 2015. Two types of BCR interactions are positively selected during leukemia development in the Eμ-TCL1 transgenic mouse model of CLL. *Blood* 125: 1578–1588.
75. Jiménez de Oya, N., M. De Giovanni, J. Fioravanti, R. Übelhart, P. Di Lucia, A. Fiocchi, S. Iacovelli, D. G. Efremov, F. Caligaris-Cappio, H. Jumaa, et al. 2017. Pathogen-specific B-cell receptors drive chronic lymphocytic leukemia by light-chain-dependent cross-reaction with autoantigens. *EMBO Mol. Med.* 9: 1482–1490.
76. Reinart, N., P. H. Nguyen, J. Boucas, N. Rosen, H. M. Kvasnicka, L. Heukamp, C. Rudolph, V. Ristovska, T. Velmans, C. Mueller, et al. 2013. Delayed development of chronic lymphocytic leukemia in the absence of macrophage migration inhibitory factor. *Blood* 121: 812–821.
77. Blair, J. E., J. D. Smilack, and S. M. Caples. 2005. Coccidioidomycosis in patients with hematologic malignancies. *Arch. Intern. Med.* 165: 113–117.
78. Forconi, F., and P. Moss. 2015. Perturbation of the normal immune system in patients with CLL. *Blood* 126: 573–581.
79. Alhakeem, S. S., M. K. McKenna, K. Z. Oben, S. K. Noothi, J. R. Rivas, G. C. Hildebrandt, R. A. Fleischman, V. M. Rangnekar, N. Muthusamy, and S. Bondada. 2018. Chronic lymphocytic leukemia-derived IL-10 suppresses antitumor immunity. *J. Immunol.* 200: 4180–4189.
80. Arruga, F., B. B. Gyau, A. Iannello, N. Vitale, T. Vaisitti, and S. Deaglio. 2020. Immune response dysfunction in chronic lymphocytic leukemia:

dissecting molecular mechanisms and microenvironmental conditions. *Int. J. Mol. Sci.* 21: 1825.
81. Kirkland, T. N., and J. Fierer. 1983. Inbred mouse strains differ in resistance to lethal *Coccidioides immitis* infection. *Infect. Immun.* 40: 912–916.
82. Fierer, J., L. Walls, F. Wright, and T. N. Kirkland. 1999. Genes influencing resistance to *Coccidioides immitis* and the interleukin-10 response map to chromosomes 4 and 6 in mice. *Infect. Immun.* 67: 2916–2919.
83. del Pilar Jiménez-A, M., S. Viriyakosol, L. Walls, S. K. Datta, T. Kirkland, S. E. Heinsbroek, G. Brown, and J. Fierer. 2008. Susceptibility to *Coccidioides* species in C57BL/6 mice is associated with expression of a truncated splice variant of Dectin-1 (Clec7a). *Genes Immun.* 9: 338–348.
84. Mead, H. L., C. C. Roe, E. A. Higgins Keppler, M. C. C. Van Dyke, K. L. Laux, A. L. Funke, K. J. Miller, H. D. Bean, J. W. Sahl, and B. M. Barker. 2020. Defining critical genes during spherule remodeling and endospore development in the fungal pathogen, *Coccidioides posadasii*. *Front. Genet.* 11: 483.
85. Patin, E. C., A. Thompson, and S. J. Orr. 2019. Pattern recognition receptors in fungal immunity. *Semin. Cell Dev. Biol.* 89: 24–33.
86. Taylor, P. R., G. D. Brown, D. M. Reid, J. A. Willment, L. Martinez-Pomares, S. Gordon, and S. Y. Wong. 2002. The β-glucan receptor, dectin-1, is predominantly expressed on the surface of cells of the monocyte/macrophage and neutrophil lineages. *J. Immunol.* 169: 3876–3882.
87. Seo, B. S., S. H. Lee, J. E. Lee, Y. C. Yoo, J. Lee, and S. R. Park. 2013. Dectin-1 stimulation selectively reinforces LPS-driven IgG1 production by mouse B cells. *Immune Netw.* 13: 205–212.
88. Viriyakosol, S., M. P. Jimenez, M. A. Gurney, M. E. Ashbaugh, and J. Fierer. 2013. Dectin-1 is required for resistance to coccidioidomycosis in mice. *MBio* 4: e00597-12.
89. Clemons, K. V., M. A. Antonysamy, M. E. Danielson, K. S. Michel, M. Martinez, V. Chen, and D. A. Stevens. 2015. Whole glucan particles as a vaccine against systemic coccidioidomycosis. *J. Med. Microbiol.* 64: 1237–1243.
90. Campuzano, A., H. Zhang, G. R. Ostroff, L. Dos Santos Dias, M. Wüthrich, B. S. Klein, J. J. Yu, H. H. Lara, J. L. Lopez-Ribot, and C. Y. Hung. 2020. CARD9-associated Dectin-1 and Dectin-2 are required for protective immunity of a multivalent vaccine against *Coccidioides posadasii* infection. *J. Immunol.* 204: 3296–3306.
91. Ramirez-Ortiz, Z. G., C. A. Specht, J. P. Wang, C. K. Lee, D. C. Bartholomeu, R. T. Gazzinelli, and S. M. Levitz. 2008. Toll-like receptor 9-dependent immune activation by unmethylated CpG motifs in *Aspergillus fumigatus* DNA. *Infect. Immun.* 76: 2123–2129.
92. Neafsey, D. E., B. M. Barker, T. J. Sharpton, J. E. Stajich, D. J. Park, E. Whiston, C. Y. Hung, C. McMahan, J. White, S. Sykes, et al. 2010. Population genomic sequencing of *Coccidioides* fungi reveals recent hybridization and transposon control. *Genome Res.* 20: 938–946.
93. Ohmomo, H., S. Komaki, K. Ono, Y. Sutoh, T. Hachiya, E. Arai, H. Fujimoto, T. Yoshida, Y. Kanai, M. Sasaki, and A. Shimizu. 2021. Evaluation of clinical formalin-fixed paraffin-embedded tissue quality for targeted-bisulfite sequencing. *Pathol. Int.* 71: 135–140.
94. Kay, J., E. Thadhani, L. Samson, and B. Engelward. 2019. Inflammation-induced DNA damage, mutations and cancer. *DNA Repair (Amst.)* 83: 102673.
95. Palacios, F., P. Moreno, P. Morande, C. Abreu, A. Correa, V. Porro, A. I. Landoni, R. Gabus, M. Giordano, G. Dighiero, et al. 2010. High expression of AID and active class switch recombination might account for a more aggressive disease in unmutated CLL patients: link with an activated microenvironment in CLL disease. *Blood* 115: 4488–4496.
96. Huemer, M., S. Rebhandl, N. Zaborsky, F. J. Gassner, S. Hainzl, L. Weiss, D. Hebenstreit, R. Greil, and R. Geisberger. 2014. AID induces intraclonal diversity and genomic damage in CD86$^+$ chronic lymphocytic leukemia cells. *Eur. J. Immunol.* 44: 3747–3757.
97. Heintel, D., E. Kroemer, D. Kienle, I. Schwarzinger, A. Gleiss, J. Schwarzmeier, R. Marculescu, T. Le, C. Mannhalter, A. Gaiger, et al.; German CLL Study Group. 2004. High expression of activation-induced cytidine deaminase (AID) mRNA is associated with unmutated IGVH gene status and unfavourable cytogenetic aberrations in patients with chronic lymphocytic leukaemia. *Leukemia* 18: 756–762.
98. Schubert, M., F. J. Gassner, M. Huemer, J. P. Höpner, E. Akimova, M. Steiner, A. Egle, R. Greil, N. Zaborsky, and R. Geisberger. 2021. AID contributes to accelerated disease progression in the TCL1 mouse transplant model for CLL. *Cancers (Basel)* 13: 2619.
99. Patten, P. E., C. C. Chu, E. Albesiano, R. N. Damle, X. J. Yan, D. Kim, L. Zhang, A. R. Magli, J. Barrientos, J. E. Kolitz, et al. 2012. IGHV-unmutated and IGHV-mutated chronic lymphocytic leukemia cells produce activation-induced deaminase protein with a full range of biologic functions. *Blood* 120: 4802–4811.
100. Zan, H., and P. Casali. 2013. Regulation of *Aicda* expression and AID activity. *Autoimmunity* 46: 83–101.
101. Lee, H., J. S. Trott, S. Haque, S. McCormick, N. Chiorazzi, and P. K. Mongini. 2010. A cyclooxygenase-2/prostaglandin E_2 pathway augments activation-induced cytosine deaminase expression within replicating human B cells. *J. Immunol.* 185: 5300–5314.
102. Chiorazzi, N., and M. Ferrarini. 2006. Evolving view of the in-vivo kinetics of chronic lymphocytic leukemia B cells. *Hematology (Am. Soc. Hematol. Educ. Program)* 2006: 273–278, 512.
103. Calissano, C., R. N. Damle, G. Hayes, E. J. Murphy, M. K. Hellerstein, C. Moreno, C. Sison, M. S. Kaufman, J. E. Kolitz, S. L. Allen, et al. 2009. In vivo intraclonal and interclonal kinetic heterogeneity in B-cell chronic lymphocytic leukemia. *Blood* 114: 4832–4842.
104. Manukyan, G., T. Papajik, P. Gajdos, Z. Mikulkova, R. Urbanova, G. Gabcova, M. Kudelka, P. Turcsányi, P. Ryznerova, V. Prochazka, and E. Kriegova. 2017. Neutrophils in chronic lymphocytic leukemia are permanently activated and have functional defects. *Oncotarget* 8: 84889–84901.
105. Podaza, E., and D. Risnik. 2019. Neglected players: tumor associated neutrophils involvement in chronic lymphocytic leukemia progression. *Oncotarget* 10: 1862–1863.
106. Gätjen, M., F. Brand, M. Grau, K. Gerlach, R. Kettritz, J. Westermann, I. Anagnostopoulos, P. Lenz, G. Lenz, U. E. Höpken, and A. Rehm. 2016. Splenic marginal zone granulocytes acquire an accentuated neutrophil B-cell helper phenotype in chronic lymphocytic leukemia. *Cancer Res.* 76: 5253–5265.
107. Ali, M. F., C. B. Driscoll, P. R. Walters, A. H. Limper, and E. M. Carmona. 2015. β-Glucan-activated human B lymphocytes participate in innate immune responses by releasing proinflammatory cytokines and stimulating neutrophil chemotaxis. *J. Immunol.* 195: 5318–5326.
108. Lande, R., D. Ganguly, V. Facchinetti, L. Frasca, C. Conrad, J. Gregorio, S. Meller, G. Chamilos, R. Sebasigari, V. Riccieri, et al. 2011. Neutrophils activate plasmacytoid dendritic cells by releasing self-DNA-peptide complexes in systemic lupus erythematosus. *Sci. Transl. Med.* 3: 73ra19.
109. Gestermann, N., J. Di Domizio, R. Lande, O. Demaria, L. Frasca, L. Feldmeyer, J. Di Lucca, and M. Gilliet. 2018. Netting neutrophils activate autoreactive B cells in lupus. *J. Immunol.* 200: 3364–3371.
110. Podaza, E., F. Sabbione, D. Risnik, M. Borge, M. B. Almejún, A. Colado, H. Fernández-Grecco, M. Cabrejo, R. F. Bezares, A. Trevani, et al. 2017. Neutrophils from chronic lymphocytic leukemia patients exhibit an increased capacity to release extracellular traps (NETs). *Cancer Immunol. Immunother.* 66: 77–89.
111. Schwaller, J., P. Schneider, P. Mhawech-Fauceglia, T. McKee, S. Myit, T. Matthes, J. Tschopp, O. Donze, F. A. Le Gal, and B. Huard. 2007. Neutrophil-derived APRIL concentrated in tumor lesions by proteoglycans correlates with human B-cell lymphoma aggressiveness. [Published erratum appears in 2007 *Blood* 110: 1474.] *Blood* 109: 331–338 .

112. Puga, I., M. Cols, C. M. Barra, B. He, L. Cassis, M. Gentile, L. Comerma, A. Chorny, M. Shan, W. Xu, et al. 2011. B cell-helper neutrophils stimulate the diversification and production of immunoglobulin in the marginal zone of the spleen. *Nat. Immunol.* 13: 170–180.
113. Parsa, R., H. Lund, A. M. Georgoudaki, X. M. Zhang, A. Ortlieb Guerreiro-Cacais, D. Grommisch, A. Warnecke, A. L. Croxford, M. Jagodic, B. Becher, et al. 2016. BAFF-secreting neutrophils drive plasma cell responses during emergency granulopoiesis. *J. Exp. Med.* 213: 1537–1553.
114. Planelles, L., C. E. Carvalho-Pinto, G. Hardenberg, S. Smaniotto, W. Savino, R. Gómez-Caro, M. Alvarez-Mon, J. de Jong, E. Eldering, C. Martínez-A, et al. 2004. APRIL promotes B-1 cell-associated neoplasm. *Cancer Cell* 6: 399–408.
115. Kocher, T., D. Asslaber, N. Zaborsky, S. Flenady, U. Denk, P. Reinthaler, M. Ablinger, R. Geisberger, J. W. Bauer, M. Seiffert, et al. 2016. $CD4^+$ T cells, but not non-classical monocytes, are dispensable for the development of chronic lymphocytic leukemia in the TCL1-tg murine model. *Leukemia* 30: 1409–1413.
116. Yona, S., K. W. Kim, Y. Wolf, A. Mildner, D. Varol, M. Breker, D. Strauss-Ayali, S. Viukov, M. Guilliams, A. Misharin, et al. 2013. Fate mapping reveals origins and dynamics of monocytes and tissue macrophages under homeostasis. [Published erratum appears in 2013 *Immunity* 38: 1073–1079.] *Immunity* 38: 79–91.
117. Gamrekelashvili, J., R. Giagnorio, J. Jussofie, O. Soehnlein, J. Duchene, C. G. Briseño, S. K. Ramasamy, K. Krishnasamy, A. Limbourg, T. Kapanadze, et al. 2016. Regulation of monocyte cell fate by blood vessels mediated by Notch signalling. *Nat. Commun.* 7: 12597.
118. Chong, S. Z., M. Evrard, S. Devi, J. Chen, J. Y. Lim, P. See, Y. Zhang, J. M. Adrover, B. Lee, L. Tan, et al. 2016. CXCR4 identifies transitional bone marrow premonocytes that replenish the mature monocyte pool for peripheral responses. *J. Exp. Med.* 213: 2293–2314.
119. Serbina, N. V., and E. G. Pamer. 2006. Monocyte emigration from bone marrow during bacterial infection requires signals mediated by chemokine receptor CCR2. *Nat. Immunol.* 7: 311–317.
120. Shi, C., T. Jia, S. Mendez-Ferrer, T. M. Hohl, N. V. Serbina, L. Lipuma, I. Leiner, M. O. Li, P. S. Frenette, and E. G. Pamer. 2011. Bone marrow mesenchymal stem and progenitor cells induce monocyte emigration in response to circulating toll-like receptor ligands. *Immunity* 34: 590–601.
121. Watanabe, S., M. Alexander, A. V. Misharin, and G. R. S. Budinger. 2019. The role of macrophages in the resolution of inflammation. *J. Clin. Invest.* 129: 2619–2628.
122. Mildner, A., J. Schönheit, A. Giladi, E. David, D. Lara-Astiaso, E. Lorenzo-Vivas, F. Paul, L. Chappell-Maor, J. Priller, A. Leutz, et al. 2017. Genomic characterization of murine monocytes reveals C/EBPβ transcription factor dependence of $Ly6C^-$ cells. *Immunity* 46: 849–862.e7.
123. Auffray, C., D. Fogg, M. Garfa, G. Elain, O. Join-Lambert, S. Kayal, S. Sarnacki, A. Cumano, G. Lauvau, and F. Geissmann. 2007. Monitoring of blood vessels and tissues by a population of monocytes with patrolling behavior. *Science* 317: 666–670.
124. Blanco, G., A. Puiggros, B. Sherry, L. Nonell, X. Calvo, E. Puigdecanet, P. Y. Chiu, Y. Kieso, G. Ferrer, F. Palacios, et al. 2021. Chronic lymphocytic leukemia-like monoclonal B-cell lymphocytosis exhibits an increased inflammatory signature that is reduced in early-stage chronic lymphocytic leukemia. *Exp. Hematol.* 95: 68–80.
125. Roessner, P. M., and M. Seiffert. 2020. T-cells in chronic lymphocytic leukemia: guardians or drivers of disease? *Leukemia* 34: 2012–2024.
126. Grioni, M., A. Brevi, E. Cattaneo, A. Rovida, J. Bordini, M. T. S. Bertilaccio, M. Ponzoni, G. Casorati, P. Dellabona, P. Ghia, et al. 2021. $CD4^+$ T cells sustain aggressive chronic lymphocytic leukemia in Eμ-TCL1 mice through a CD40L-independent mechanism. *Blood Adv.* 5: 2817–2828.
127. Rivas, J. R., Y. Liu, S. S. Alhakeem, J. M. Eckenrode, F. Marti, J. P. Collard, Y. Zhang, K. A. Shaaban, N. Muthusamy, G. C. Hildebrandt, et al. 2021. Interleukin-10 suppression enhances T-cell antitumor immunity and responses to checkpoint blockade in chronic lymphocytic leukemia. *Leukemia* 35: 3188–3200.
128. Smith, L. K., G. M. Boukhaled, S. A. Condotta, S. Mazouz, J. J. Guthmiller, R. Vijay, N. S. Butler, J. Bruneau, N. H. Shoukry, C. M. Krawczyk, and M. J. Richer. 2018. Interleukin-10 directly inhibits $CD8^+$ T cell function by enhancing N-glycan branching to decrease antigen sensitivity. *Immunity* 48: 299–312.e5.
129. Nunes, C., R. Wong, M. Mason, C. Fegan, S. Man, and C. Pepper. 2012. Expansion of a $CD8^+PD\text{-}1^+$ replicative senescence phenotype in early stage CLL patients is associated with inverted CD4:CD8 ratios and disease progression. *Clin. Cancer Res.* 18: 678–687.
130. Riches, J. C., J. K. Davies, F. McClanahan, R. Fatah, S. Iqbal, S. Agrawal, A. G. Ramsay, and J. G. Gribben. 2013. T cells from CLL patients exhibit features of T-cell exhaustion but retain capacity for cytokine production. *Blood* 121: 1612–1621.
131. Hofbauer, J. P., C. Heyder, U. Denk, T. Kocher, C. Holler, D. Trapin, D. Asslaber, I. Tinhofer, R. Greil, and A. Egle. 2011. Development of CLL in the TCL1 transgenic mouse model is associated with severe skewing of the T-cell compartment homologous to human CLL. *Leukemia* 25: 1452–1458.
132. Greten, F. R., and S. I. Grivennikov. 2019. Inflammation and cancer: triggers, mechanisms, and consequences. *Immunity* 51: 27–41.
133. Stevens, W. B., M. G. Netea, A. P. Kater, and W. J. van der Velden. 2016. "Trained immunity": consequences for lymphoid malignancies. *Haematologica* 101: 1460–1468.
134. Nejman, D., I. Livyatan, G. Fuks, N. Gavert, Y. Zwang, L. T. Geller, A. Rotter-Maskowitz, R. Weiser, G. Mallel, E. Gigi, et al. 2020. The human tumor microbiome is composed of tumor type-specific intracellular bacteria. *Science* 368: 973–980.
135. Riquelme, E., Y. Zhang, L. Zhang, M. Montiel, M. Zoltan, W. Dong, P. Quesada, I. Sahin, V. Chandra, A. San Lucas, et al. 2019. Tumor microbiome diversity and composition influence pancreatic cancer outcomes. *Cell* 178: 795–806.e12.
136. Schöllkopf, C., M. Melbye, L. Munksgaard, K. E. Smedby, K. Rostgaard, B. Glimelius, E. T. Chang, G. Roos, M. Hansen, H. O. Adami, and H. Hjalgrim. 2008. *Borrelia* infection and risk of non-Hodgkin lymphoma. *Blood* 111: 5524–5529.
137. Cerhan, J. R., and T. M. Habermann. 2021. Epidemiology of marginal zone lymphoma. *Ann. Lymphoma* 5: 1.
138. Smedby, K. E., and M. Ponzoni. 2017. The aetiology of B-cell lymphoid malignancies with a focus on chronic inflammation and infections. *J. Intern. Med.* 282: 360–370.
139. Cristofori, F., V. N. Dargenio, C. Dargenio, V. L. Miniello, M. Barone, and R. Francavilla. 2021. Anti-inflammatory and immunomodulatory effects of probiotics in gut inflammation: a door to the body. *Front. Immunol.* 12: 578386.